

# 000 001 002 003 004 005 006 007 008 009 010 011 012 013 014 015 016 017 018 019 020 021 022 023 024 025 026 027 028 029 030 031 032 033 034 035 036 037 038 039 040 041 042 043 044 045 046 047 048 049 050 051 052 053 REPRESENTATION CONVERGENCE: MUTUAL DISTIL- LATION IS SECRETLY A FORM OF REGULARIZATION

Anonymous authors

Paper under double-blind review

## ABSTRACT

In this paper, we argue that mutual distillation between reinforcement learning policies serves as an *implicit regularization*, preventing them from overfitting to irrelevant features. We highlight two *separate* contributions: (i) Theoretically, for the first time, we provide an *end-to-end* theoretical proof that enhancing the policy robustness to irrelevant features leads to improved generalization performance. (ii) Empirically, we demonstrate that mutual distillation between policies contributes to such robustness, enabling the spontaneous emergence of *invariant representations* over pixel inputs. Ultimately, we do not claim to achieve state-of-the-art performance but rather focus on uncovering the underlying principles of generalization and deepening our understanding of its mechanisms. Our website: <https://dml-rl.github.io/>.

## 1 INTRODUCTION

Humans exhibit a remarkable ability to learn robustly and generalize across diverse environments. Once a skill is acquired, it often transfers seamlessly to new contexts that share the same underlying semantics, even when their visual appearance differs substantially. For example, consider a person who becomes proficient at a video game, even if the background graphics or character textures are altered, the player retains their ability to perform well, effortlessly adapting to the new setting. This suggests that human learning is not overly dependent on low-level visual details, but rather grounded in abstract representations that capture the essential structure of a task. Neuroscientific studies support this view, linking abstract reasoning to the human prefrontal cortex (Bengtsson et al., 2009; Dumontheil, 2014), and highlighting the role of inhibitory neurons in enhancing cognitive processing efficiency (Pi et al., 2013).

In stark contrast, visual reinforcement learning (VRL) agents often struggle with generalization. While they can be trained to solve complex tasks in specific environments, even minor changes, such as shifts in color schemes or background textures, can significantly degrade their performance. This sensitivity indicates that VRL agents tend to overfit to superficial visual features, failing to capture the underlying structure of the task (Cobbe et al., 2019; 2020). These limitations give rise to a fundamental question:

*What hinders reinforcement learning agents from generalizing like humans? How can we enable them to learn robust representations that drive human-like generalization behavior?*

The core reason behind the limited generalization ability of VRL agents lies in their reliance on convolutional neural networks (CNNs) as visual encoders. While CNNs are the de facto choice for processing high-dimensional visual inputs, they are notoriously sensitive to even small perturbations (Goodfellow et al., 2014). This brittleness significantly hampers the robustness of learned policies and limits their ability to generalize. To address this issue, one common strategy is to apply data augmentation (Shorten & Khoshgoftaar, 2019), which improves robustness by diversifying the training distribution and reducing dataset-induced biases. Alternatively, invariant representation learning has emerged as a principled approach to tackle generalization problem from a feature-learning perspective. It aims to extract representations that remain stable under a wide range of input transformations, thereby promoting robustness and transferability (Nguyen et al., 2021).

While data augmentation is an effective bias mitigation technique, its reliance on task-specific strategies that are manually crafted by human experts, poses a challenge for designing task-independent

054 solutions. In contrast, our method enables agents to generalize without any handcrafted augmentations or external priors, relying purely on training experience. Invariant representation learning  
 055 is a promising approach to enhance model’s cross-domain generalization. However, it relies on  
 056 transformation correspondences, which are fundamentally inaccessible in the generalization scenarios  
 057 of reinforcement learning due to the dynamic nature of environments. In addition, the invariant  
 058 representation framework inherently separates the encoder from the model, unnecessarily complicating  
 059 the theoretical analysis. Instead, our framework is theoretically and empirically end-to-end.  
 060

061 In this paper, we first propose a novel theoretical framework to analyze the generalization problem  
 062 in reinforcement learning and show that the policy robustness to irrelevant features enhances its  
 063 generalization performance. Building upon this principled insight, we then provide empirical evidence  
 064 that deep mutual learning (DML) (Zhang et al., 2018b) can implicitly prevent online RL policies  
 065 from overfitting to such irrelevant features, leading to a stable learning process and significant  
 066 generalization improvements.

067 In summary, the main contributions of this paper are as follows:  
 068

- 069 • We theoretically prove that improving the policy robustness to irrelevant features enhances  
 070 its generalization performance. To the best of our knowledge, we are the first to provide a  
 071 rigorous proof of this intuition.
- 072 • We propose a hypothesis that deep mutual learning (DML) enhances the generalization  
 073 performance of the policy by implicitly regularizing irrelevant features. We also provide  
 074 intuitive insights to support this hypothesis.
- 075 • Strong empirical results support our theory and hypothesis, showing that DML technique  
 076 leads to consistent improvements in generalization performance.

## 078 2 RELATED WORK

080 **The generalization of deep reinforcement learning** has been widely studied, and previous work has  
 081 pointed out the overfitting problem in deep reinforcement learning (Rajeswaran et al., 2017; Zhang  
 082 et al., 2018a; Justesen et al., 2018; Packer et al., 2018; Song et al., 2019; Cobbe et al., 2019; Grigsby  
 083 & Qi, 2020; Cobbe et al., 2020; Yuan et al., 2023; Suau et al., 2023; Kirk et al., 2023). A natural  
 084 approach to avoid the overfitting problem is to apply regularization techniques originally developed  
 085 for supervised learning such as dropout (Srivastava et al., 2014; Farebrother et al., 2018; Igl et al.,  
 086 2019), data augmentation (Laskin et al., 2020; Yarats et al., 2021; Zhang & Guo, 2021; Raileanu  
 087 et al., 2021; Ma et al., 2022), domain randomization (Tobin et al., 2017; Yue et al., 2019; Slaoui et al.,  
 088 2019; Lee et al., 2019; Mehta et al., 2020). On the other hand, in order to improve sample efficiency,  
 089 previous studies encouraged the policy network and value network to share parameters (Schulman  
 090 et al., 2017; Huang et al., 2022). However, recent works have explored the idea of decoupling the  
 091 two and proposed additional distillation strategies (Cobbe et al., 2021; Raileanu & Fergus, 2021;  
 092 Moon et al., 2022). In particular, Raileanu & Fergus (2021) demonstrated that more information is  
 093 needed to accurately estimate the value function, which can lead to overfitting. Moreover, exploration  
 094 has also been shown to be an effective technique for improving policy generalization (Jiang et al.,  
 095 2023; Weltevrede et al., 2024), as the exploration phase effectively alters the initial state distribution  
 096 and allows the policy to access more diverse trajectories (Weltevrede et al., 2024). In addition, prior  
 097 works also adopt kernel complexity (Yeh et al., 2023) or causal learning perspectives (Kallus & Zhou,  
 098 2020; Suau et al., 2023) as measures of representation capacity.

099 **Representation learning** is another tool for improving generalization. Prior work has either leveraged  
 100 bisimulation metrics to capture invariances by comparing states in terms of their reward and transition  
 101 distributions (Zhang et al., 2020), or adopted self-supervised objectives that align trajectories based on  
 102 behavioral similarity (Mazoure et al., 2021), which enable the encoder to learn visually robust features  
 103 without relying on explicit reward signals. However, these methods introduce an additional encoder  
 104 pretraining stage that is separate from the reinforcement learning process, potentially hindering  
 105 sample efficiency and leading to suboptimal downstream representations, which can further limit  
 106 end-to-end adaptability. Moreover, modern policy gradient algorithms such as TRPO (Schulman et al.,  
 107 2015), PPO (Schulman et al., 2017), and SPO (Xie et al., 2025) typically formulate an end-to-end  
 108 policy  $\pi$ , this further motivates us to develop a framework that is both theoretically and empirically  
 109 end-to-end, while allowing easy integration into the reinforcement learning pipeline.

108 **Knowledge distillation** is a learning paradigm that aims to align the student network with the teacher  
 109 network to achieve knowledge transfer. A commonly used practice is to distill the knowledge learned  
 110 by a large model into a smaller model to reduce inference costs after deployment (Xu et al., 2024). On  
 111 the other hand, distillation technique can also be used to distill a model with privileged information  
 112 into a model with access to only partial information to improve its generalization ability. However,  
 113 research has shown that knowledge distillation can also be applied to multiple student networks  
 114 during training to encourage them to learn from each other, called deep mutual learning (DML)  
 115 (Zhang et al., 2018b). Lai et al. (2020) then propose dual policy distillation, a student-student mutual  
 116 distillation framework that can improve performance without requiring a pre-trained teacher. Building  
 117 upon this observation, Zhao & Hospedales (2021) further demonstrate that DML can improve the  
 118 generalization performance of reinforcement learning agents, yet no in-depth analysis of why this  
 119 happens. In addition, recent studies suggest that aligning the student networks at the output layer  
 120 may be suboptimal, and recommend alignment at the logits layer instead (Deckers et al., 2024;  
 121 Vandersmissen et al.). Furthermore, Weltevrede et al. (2025) show that distilling multiple RL policies  
 122 into an ensemble on diverse training states can significantly improve zero-shot generalization, yet  
 123 their settings are limited to environments with rotational symmetry. We extend mutual distillation as  
 124 a form of regularization and propose a more general end-to-end generalization theory.

### 3 PRELIMINARIES

125 In this section, we introduce reinforcement learning under the generalization setting in Section 3.1,  
 126 as well as the DML technique in Section 3.2.

#### 3.1 MARKOV DECISION PROCESS AND GENERALIZATION

127 Markov decision process (MDP) is a mathematical framework for sequential decision-making, which  
 128 is defined by a tuple  $\mathcal{M} = (\mathcal{S}, \mathcal{A}, r, \mathcal{P}, \rho, \gamma)$ , where  $\mathcal{S}$  and  $\mathcal{A}$  represent the state space and action  
 129 space,  $r : \mathcal{S} \times \mathcal{A} \mapsto \mathbb{R}$  is the reward function,  $\mathcal{P} : \mathcal{S} \times \mathcal{A} \times \mathcal{S} \mapsto [0, 1]$  is the dynamics,  $\rho : \mathcal{S} \mapsto [0, 1]$   
 130 is the initial state distribution, and  $\gamma \in (0, 1)$  is the discount factor.

131 Define a policy  $\mu : \mathcal{S} \times \mathcal{A} \mapsto [0, 1]$ , the action-value function and value function are defined as

$$132 \quad Q^\mu(s_t, a_t) = \mathbb{E}_\mu \left[ \sum_{k=0}^{\infty} \gamma^k r(s_{t+k}, a_{t+k}) \right], \quad V^\mu(s_t) = \mathbb{E}_{a_t \sim \mu(\cdot|s_t)} [Q^\mu(s_t, a_t)]. \quad (1)$$

133 Given  $Q^\mu$  and  $V^\mu$ , the advantage function can be expressed as  $A^\mu(s_t, a_t) = Q^\mu(s_t, a_t) - V^\mu(s_t)$ .

134 In our generalization setting, we introduce a rendering function (Smallwood & Sondik, 1973)  
 135  $f : \mathcal{S} \mapsto \mathcal{O}_f \subset \mathcal{O}$  to obfuscate the agent's actual observations, which is a bijection<sup>1</sup> from  $\mathcal{S}$  to  $\mathcal{O}_f$ .  
 136 We now define the MDP induced by the underlying MDP  $\mathcal{M}$  and the rendering function  $f$ , denote it  
 137 as  $\mathcal{M}_f = (\mathcal{O}_f, \mathcal{A}, r_f, \mathcal{P}_f, \rho_f, \gamma)$ , where  $\mathcal{O}_f$  represents the observation space,  $r_f : \mathcal{O}_f \times \mathcal{A} \mapsto \mathbb{R}$  is  
 138 the reward function,  $\mathcal{P}_f : \mathcal{O}_f \times \mathcal{A} \times \mathcal{O}_f \mapsto [0, 1]$  is the dynamics, and  $\rho_f : \mathcal{O}_f \mapsto [0, 1]$  is the initial  
 139 observation distribution. We present the following assumptions:

140 **Assumption 3.1.** Assume that  $f$  can be sampled from a distribution  $p : \mathcal{F} \mapsto [0, 1]$ , where  $f \in \mathcal{F}$ ,  
 141 which means that  $\int_{\mathcal{F}} p(f) df = 1$  is naturally satisfied.

142 **Assumption 3.2.** Given any  $f \in \mathcal{F}$ ,  $o_0^f, o_t^f, o_{t+1}^f \in \mathcal{O}_f$  and  $a_t \in \mathcal{A}$ , assume that  $r_f(o_t^f, a_t) =$   
 143  $r(f^{-1}(o_t^f), a_t)$ ,  $\mathcal{P}_f(o_{t+1}^f | o_t^f, a_t) = \mathcal{P}(f^{-1}(o_{t+1}^f) | f^{-1}(o_t^f), a_t)$ ,  $\rho_f(o_0^f) = \rho(f^{-1}(o_0^f))$ .

144 **Explanation.** Assumption 3.2 states that all  $\mathcal{M}_f$  share a common underlying MDP  $\mathcal{M}$ , in which  
 145 the agent's observations are perturbed by different rendering functions while all other components  
 146 remain unchanged, much like different painters depicting the same scene in their own styles.

147 Next, consider an agent interacting with  $\mathcal{M}_f$  following the policy  $\pi : \mathcal{O} \times \mathcal{A} \mapsto [0, 1]$  to obtain a  
 148 trajectory

$$149 \quad \tau_f = (o_0^f, a_0, r_0^f, o_1^f, a_1, r_1^f, \dots, o_t^f, a_t, r_t^f, \dots), \quad (2)$$

150 <sup>1</sup>We define  $\mathcal{O}_f := \{f(s) | s \in \mathcal{S}\}$ , which means for any  $s_1 \neq s_2$ , we have  $f(s_1) \neq f(s_2)$ .

162 where  $o_0^f \sim \rho_f(\cdot)$ ,  $a_t \sim \pi(\cdot|o_t^f)$ ,  $r_t^f = r_f(o_t^f, a_t)$  and  $o_{t+1}^f \sim \mathcal{P}_f(\cdot|o_t^f, a_t)$ , we simplify the notation  
 163 to  $\tau_f \sim \pi$ . During training, the agent is only allowed to access a subset of all MDPs, which is  
 164  $\{\mathcal{M}_f | f \in \mathcal{F}_{\text{train}} \subset \mathcal{F}\}$ , and then tests its generalization performance across all MDPs. Thus, denote  
 165  $p_{\text{train}} : \mathcal{F}_{\text{train}} \mapsto [0, 1]$  as the distribution over  $\mathcal{F}_{\text{train}}$ , the agent's training performance  $\eta(\pi)$  and  
 166 generalization performance  $\zeta(\pi)$  can be expressed as

$$167 \eta(\pi) = \mathbb{E}_{f \sim p_{\text{train}}(\cdot), \tau_f \sim \pi} \left[ \sum_{t=0}^{\infty} \gamma^t r_f(o_t^f, a_t) \right], \quad \zeta(\pi) = \mathbb{E}_{f \sim p(\cdot), \tau_f \sim \pi} \left[ \sum_{t=0}^{\infty} \gamma^t r_f(o_t^f, a_t) \right]. \quad (3)$$

170 The goal of the agent is to learn a policy  $\pi$  that maximizes the generalization performance  $\zeta(\pi)$ .  
 171

### 172 3.2 DEEP MUTUAL LEARNING

174 Deep mutual learning (DML) (Zhang et al., 2018b) is a mutual distillation technique in supervised  
 175 learning. Unlike the traditional teacher-student distillation strategy, DML aligns the probability  
 176 distributions of multiple student networks by minimizing the KL divergence loss during training,  
 177 allowing them to learn from each other. Specifically,

$$178 \mathcal{L}_{\text{DML}} = \mathcal{L}_{\text{SL}} + \alpha \mathcal{L}_{\text{KL}}, \quad (4)$$

179 where  $\mathcal{L}_{\text{SL}}$  and  $\mathcal{L}_{\text{KL}}$  represent the supervised learning loss and the KL divergence loss, respectively,  
 180  $\alpha$  is the weight. Using DML, the student cohort effectively pools their collective estimate of the next  
 181 most likely classes. Finding out and matching the other most likely classes for each training instance  
 182 according to their peers increases each student's posterior entropy, which helps them converge to a  
 183 more robust representation, leading to better generalization.  
 184

## 185 4 THEORETICAL RESULTS

187 In this section, we present the main results of this paper, demonstrating that enhancing the agent's  
 188 robustness to irrelevant features will improve its generalization performance.  
 189

190 A key issue is that we do not exactly know the probability distribution  $p_{\text{train}}$ . Note that  $\mathcal{F}_{\text{train}}$  is  
 191 a subset of  $\mathcal{F}$ , we naturally assume that the probability distribution  $p_{\text{train}}$  can be derived from the  
 192 normalized probability distribution  $p$ .

193 **Assumption 4.1.** For any  $f \in \mathcal{F}$ , assume that

$$194 p_{\text{train}}(f) = \frac{p(f) \cdot \mathbb{I}(f \in \mathcal{F}_{\text{train}})}{Z}, \quad p_{\text{eval}}(f) = \frac{p(f) \cdot \mathbb{I}(f \in \mathcal{F}_{\text{eval}})}{1 - Z}, \quad (5)$$

197 where  $Z = \int_{\mathcal{F}_{\text{train}}} p(f) df$  and  $1 - Z$  is the normalization term,  $\mathcal{F}_{\text{eval}} = \mathcal{F} - \mathcal{F}_{\text{train}}$ ,  $\mathbb{I}(\cdot)$  denotes  
 198 the indicator function.

199 An interesting fact is that, for a specific policy  $\pi$ , if we only consider its interaction with  $\mathcal{M}_f$ , we  
 200 can establish a bijection between this policy and a certain underlying policy that directly interacts  
 201 with  $\mathcal{M}$ . We now denote it as  $\mu_f(\cdot|s_t) = \pi(\cdot|f(s_t))$ . By further defining the normalized discounted  
 202 visitation distribution  $d^{\mu}(s) = (1 - \gamma) \sum_{t=0}^{\infty} \gamma^t \mathbb{P}(s_t = s|\mu)$ , we can use this underlying policy  $\mu_f$   
 203 to replace the training and generalization performance of the policy  $\pi$ . Specifically, we have the  
 204 following connection:

205 **Lemma 4.2.** For any given policy  $\pi$ , define its underlying policy as  $\mu_f(\cdot|s_t) = \pi(\cdot|f(s_t))$ , then

$$207 \eta(\pi) = \frac{1}{1 - \gamma} \mathbb{E}_{\substack{f \sim p_{\text{train}}(\cdot) \\ s \sim d^{\mu_f}(\cdot) \\ a \sim \mu_f(\cdot|s)}} [r(s, a)], \quad \zeta(\pi) = \frac{1}{1 - \gamma} \mathbb{E}_{\substack{f \sim p(\cdot) \\ s \sim d^{\mu_f}(\cdot) \\ a \sim \mu_f(\cdot|s)}} [r(s, a)]. \quad (6)$$

211 *Proof.* See Appendix F.1. □  
 212

213 We can thus analyze the generalization problem using the underlying policy  $\mu_f$ . Then, we define  
 214  $L_{\pi}(\tilde{\pi}) = \eta(\pi) + \frac{1}{1 - \gamma} \mathbb{E}_{\substack{f \sim p_{\text{train}}(\cdot), s \sim d^{\mu_f}(\cdot), a \sim \mu_f(\cdot|s)}} [A^{\mu_f}(s, a)]$  as the first-order approximation of  $\eta$   
 215 (Schulman et al., 2015), we can derive the following lower bounds:

216  
217 **Theorem 4.3** (Training performance lower bound). *Given any two policies,  $\tilde{\pi}$  and  $\pi$ , the following  
218 bound holds:*

$$219 \quad \eta(\tilde{\pi}) \geq L_{\pi}(\tilde{\pi}) - \frac{2\gamma\epsilon_{\text{train}}}{(1-\gamma)^2} \mathbb{E}_{\substack{f \sim p_{\text{train}}(\cdot) \\ s \sim d^{\mu_f}(\cdot)}} [D_{\text{TV}}(\tilde{\mu}_f \| \mu_f)[s]], \quad (7)$$

220  
221 where  $\epsilon_{\text{train}} = \max_{f \in \mathcal{F}_{\text{train}}} \{ \max_s |\mathbb{E}_{a \sim \tilde{\mu}_f(\cdot|s)} [A^{\mu_f}(s, a)]| \}.$

223 *Proof.* See Appendix F.3. □

225 **Theorem 4.4** (Generalization performance lower bound). *Given any two policies,  $\tilde{\pi}$  and  $\pi$ , the  
226 following bound holds:*

$$227 \quad \zeta(\tilde{\pi}) \geq L_{\pi}(\tilde{\pi}) - \frac{2r_{\max}(1-Z)}{1-\gamma} - \frac{2\gamma\epsilon_{\text{train}}}{(1-\gamma)^2} \mathbb{E}_{\substack{f \sim p_{\text{train}}(\cdot) \\ s \sim d^{\mu_f}(\cdot)}} [D_{\text{TV}}(\tilde{\mu}_f \| \mu_f)[s]] \\ 228 \quad - \frac{2\delta_{\text{train}}(1-Z)}{1-\gamma} \mathbb{E}_{\substack{f \sim p_{\text{train}}(\cdot) \\ s \sim d^{\tilde{\mu}_f}(\cdot)}} [D_{\text{TV}}(\tilde{\mu}_f \| \mu_f)[s]] - \frac{2\delta_{\text{eval}}(1-Z)}{1-\gamma} \mathbb{E}_{\substack{f \sim p_{\text{eval}}(\cdot) \\ s \sim d^{\tilde{\mu}_f}(\cdot)}} [D_{\text{TV}}(\tilde{\mu}_f \| \mu_f)[s]], \quad (8)$$

235 where  $r_{\max} = \max_{s,a} |r(s, a)|$ ,  $\delta_{\text{train}} = \max_{f \in \mathcal{F}_{\text{train}}} \{ \max_{s,a} |A^{\mu_f}(s, a)| \}$ , and  $\delta_{\text{eval}} =$   
236  $\max_{f \in \mathcal{F}_{\text{eval}}} \{ \max_{s,a} |A^{\mu_f}(s, a)| \}$ .

238 *Proof.* See Appendix F.2. □

240 **Explanation.** Building upon Theorems 4.3 and 4.4, we observe that, in contrast to the lower bound  
241 on training performance, the lower bound on generalization performance incorporates three additional  
242 terms, scaled by the common coefficient  $(1 - Z)$ . This implies that increasing  $Z$  contributes to  
243 improved generalization performance, with the special case of  $Z = 1$  resulting in alignment between  
244 generalization and training performance. Notably, this theoretical insight was also validated in Figure  
245 2 of Cobbe et al. (2020).

246 However, once the training level is fixed (i.e.,  $\mathcal{F}_{\text{train}}$ ),  $Z$  is a constant, improving generalization  
247 performance requires constraining the following three terms:

$$248 \quad \underbrace{\mathbb{E}_{\substack{f \sim p_{\text{train}}(\cdot) \\ s \sim d^{\tilde{\mu}_f}(\cdot)}} [D_{\text{TV}}(\tilde{\mu}_f \| \mu_f)[s]]}_{\text{denote it as } \mathfrak{D}_1}, \underbrace{\mathbb{E}_{\substack{f \sim p_{\text{eval}}(\cdot) \\ s \sim d^{\tilde{\mu}_f}(\cdot)}} [D_{\text{TV}}(\tilde{\mu}_f \| \mu_f)[s]]}_{\text{denote it as } \mathfrak{D}_2}, \underbrace{\mathbb{E}_{\substack{f \sim p_{\text{train}}(\cdot) \\ s \sim d^{\mu_f}(\cdot)}} [D_{\text{TV}}(\tilde{\mu}_f \| \mu_f)[s]]}_{\text{denote it as } \mathfrak{D}_{\text{train}}}. \quad (9)$$

253 During the training process, we can only empirically bound  $\mathfrak{D}_{\text{train}}$ . Next, we establish the upper  
254 bounds of  $\mathfrak{D}_1$  and  $\mathfrak{D}_2$ . Specifically, we propose the following theorem:

255 **Theorem 4.5.** *Given any two policies,  $\tilde{\pi}$  and  $\pi$ , the following bound holds:*

$$256 \quad \mathfrak{D}_1 \leq \left(1 + \frac{2\gamma\sigma_{\text{train}}}{1-\gamma}\right) \mathfrak{D}_{\text{train}}, \quad \mathfrak{D}_2 \leq \left(1 + \frac{2\gamma\sigma_{\text{eval}}}{1-\gamma}\right) \underbrace{\mathbb{E}_{\substack{f \sim p_{\text{eval}}(\cdot) \\ s \sim d^{\mu_f}(\cdot)}} [D_{\text{TV}}(\tilde{\mu}_f \| \mu_f)[s]]}_{\text{denote it as } \mathfrak{D}_{\text{eval}}}, \quad (10)$$

261 where  $\sigma_{\text{train}} = \max_{f \in \mathcal{F}_{\text{train}}} \{ D_{\text{TV}}^{\max}(\tilde{\mu}_f \| \mu_f)[s] \}$  and  $\sigma_{\text{eval}} = \max_{f \in \mathcal{F}_{\text{eval}}} \{ D_{\text{TV}}^{\max}(\tilde{\mu}_f \| \mu_f)[s] \}$ ,  
262  $D_{\text{TV}}^{\max}(\tilde{\mu}_f \| \mu_f)[s]$  is defined as  $\max_s D_{\text{TV}}(\tilde{\mu}_f \| \mu_f)[s]$ .

264 *Proof.* See Appendix F.4. □

266 The only problem now is finding the relationship between  $\mathfrak{D}_{\text{eval}}$  and  $\mathfrak{D}_{\text{train}}$ . To achieve this, we  
267 would like to first introduce the following definition, which represents the policy robustness to  
268 irrelevant features.

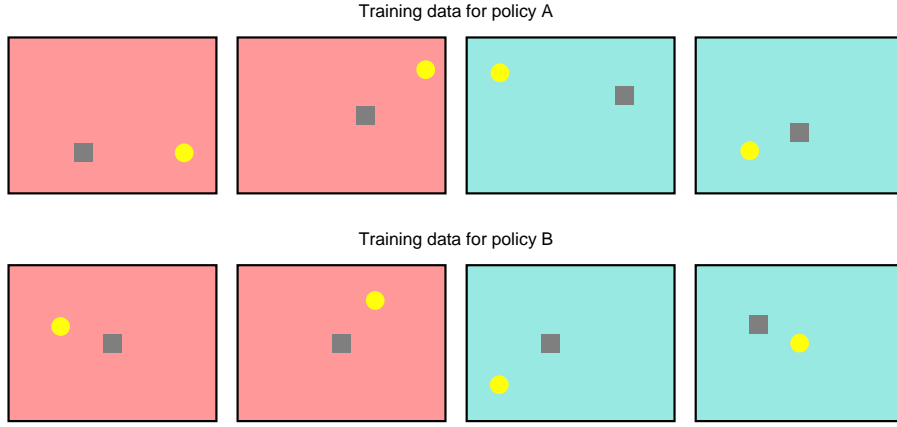


Figure 1: This is a toy environment where the gray agent's goal is to pick up coins.

**Definition 4.6** ( $\mathcal{R}$ -robust). We say that the policy  $\pi$  is  $\mathcal{R}$ -robust if it satisfies

$$\sup_{s \in \mathcal{S}, \tilde{f}, f \in \mathcal{F}} D_{\text{TV}}(\mu_{\tilde{f}} \| \mu_f)[s] = \mathcal{R}. \quad (11)$$

**Explanation.** This definition demonstrates how the policy  $\pi$  is influenced by two different rendering functions,  $\tilde{f}$  and  $f$ , for any given underlying state  $s$ . If  $\mathcal{R} = 0$ , it indicates that  $D_{\text{TV}}(\mu_{\tilde{f}} \| \mu_f)[s] \equiv 0$ , which means that the policy is no longer affected by any irrelevant features.

Our intention in this definition is not to derive the tightest possible bound but rather to demonstrate how policy robustness to irrelevant features can contribute to improved generalization. Subsequently, leveraging Definition 4.6, we establish an upper bound for  $\mathfrak{D}_{\text{eval}}$ .

**Theorem 4.7.** Given any two policies,  $\tilde{\pi}$  and  $\pi$ , assume that  $\tilde{\pi}$  is  $\mathcal{R}_{\tilde{\pi}}$ -robust, and  $\pi$  is  $\mathcal{R}_{\pi}$ -robust, then the following bound holds:

$$\mathfrak{D}_{\text{eval}} \leq \left(1 + \frac{2\gamma\sigma_{\text{train}}}{1-\gamma}\right) \mathcal{R}_{\pi} + \mathcal{R}_{\tilde{\pi}} + \mathfrak{D}_{\text{train}}. \quad (12)$$

*Proof.* See Appendix F.5. □

Altogether, by combining Theorems 4.4, 4.5, and 4.7, we can derive the following corollary:

**Corollary 4.8.** Given any two policies,  $\tilde{\pi}$  and  $\pi$ , the following bound holds:

$$\zeta(\tilde{\pi}) \geq L_{\pi}(\tilde{\pi}) - C_{\text{train}}\mathfrak{D}_{\text{train}} - C_{\pi}\mathcal{R}_{\pi} - C_{\tilde{\pi}}\mathcal{R}_{\tilde{\pi}} - C, \quad (13)$$

where

$$\begin{aligned} C_{\text{train}} &= \frac{2\delta_{\text{train}}(1-Z)}{1-\gamma} \left(1 + \frac{2\gamma\sigma_{\text{train}}}{1-\gamma}\right) + \frac{2\delta_{\text{eval}}(1-Z)}{1-\gamma} \left(1 + \frac{2\gamma\sigma_{\text{eval}}}{1-\gamma}\right) + \frac{2\gamma\epsilon_{\text{train}}}{(1-\gamma)^2}, \\ C_{\pi} &= \frac{2\delta_{\text{eval}}(1-Z)}{1-\gamma} \left(1 + \frac{2\gamma\sigma_{\text{eval}}}{1-\gamma}\right) \left(1 + \frac{2\gamma\sigma_{\text{train}}}{1-\gamma}\right), \\ C_{\tilde{\pi}} &= \frac{2\delta_{\text{eval}}(1-Z)}{1-\gamma} \left(1 + \frac{2\gamma\sigma_{\text{eval}}}{1-\gamma}\right), \quad C = \frac{2r_{\max}(1-Z)}{1-\gamma}. \end{aligned} \quad (14)$$

**Explanation.** This represents our central theoretical result, demonstrating that enhancing generalization performance requires not only minimizing  $\mathfrak{D}_{\text{train}}$  during training but also improving policy robustness to irrelevant features, specifically by reducing  $\mathcal{R}_{\pi}$  and  $\mathcal{R}_{\tilde{\pi}}$ . Furthermore, we emphasize that these results rely solely on the mild Assumptions 3.1, 3.2, and 4.1. Consequently, this constitutes a novel contribution that is broadly applicable to a wide range of algorithms.

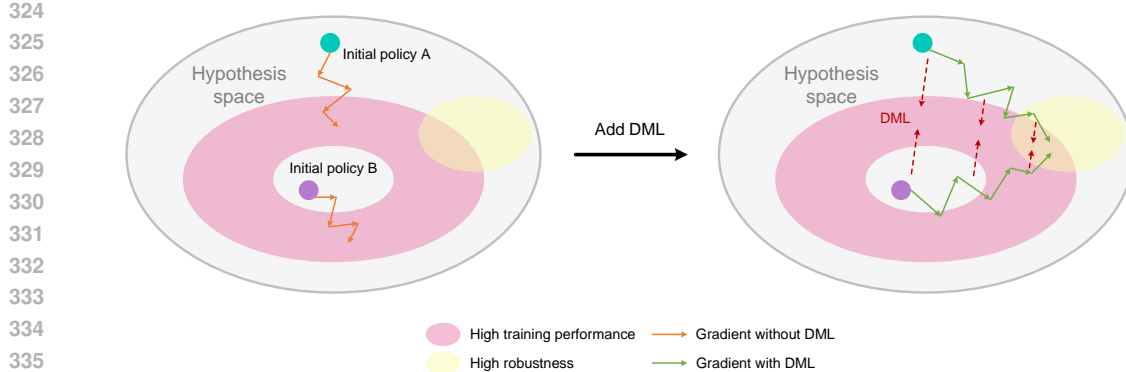


Figure 2: (Left) Independently trained reinforcement learning policies may overfit to irrelevant features. (Right) Through mutual distillation via DML, two policies regularize each other to converge toward a more robust hypothesis space, ultimately improving generalization performance.

## 5 DISTILLATION AS REGULARIZATION

Despite the theoretical advancements, in typical generalization settings, both the underlying MDP and the rendering function remain unknown. Next, we begin by introducing a minimal toy example in Section 5.1, which we then provide an in-depth analyze in Section 5.2 to motivate our hypothesis.

### 5.1 TOY EXAMPLE

Let's consider a simple environment where the agent attempts to pick up coins to earn rewards (see Figure 1). The agent's observations are the current pixels. It is clear that the agent's true objective is to pick up the coins, and the background color is a spurious feature. However, upon observing the training data for policy A, we can see that in the red background, the coins are always on the right side of the agent, while in the cyan background, the coins are always on the left side. As a result, when training policy A using reinforcement learning algorithms, it is likely to exhibit overfitting behavior, such as moving to the right in a red background and to the left in a cyan background.

However, the overfitting of policy A to the background color will fail in the training data of policy B, because in policy B's training data, regardless of whether the background color is red or cyan, the coin can appear either on the left or right side of the agent. Therefore, through DML, policy A is regularized by the behavior of policy B, effectively preventing policy A from overfitting to the background color. In other words, any irrelevant features learned by policy A could lead to suboptimal performance of policy B, and vice versa. Thus, we hypothesize that this process will force both policies to learn the true underlying semantics, ultimately improving generalization performance.

### 5.2 HYPOTHESIS

Motivated by Section 5.1, DML can be viewed as a form of implicit regularization against irrelevant features, as demonstrated in Figure 2, which illustrates two randomly initialized policies independently trained using reinforcement learning algorithms. In this case, since the training samples only include a portion of all possible MDPs, the policies are likely to overfit to irrelevant features and fail to converge to a robust hypothesis space.

Applying DML to the training process of both policies facilitates mutual learning, which can mitigate overfitting to irrelevant features. Due to the randomness of parameter initialization and the interaction process, they generate different training samples, DML encourages both policies to make consistent decisions based on the same observations. As discussed in Section 5.1, any irrelevant features learned by policy A are likely to degrade the performance of policy B, and vice versa. As training progresses, DML will drive both policies to learn more meaningful and useful representations, gradually reducing the divergence between them. Ideally, we hypothesize that both policies will capture the essential aspects of high-dimensional observations as time grows.

378 

## 6 EXPERIMENTS

380 This section presents our main empirical results. Section 6.1 introduces the implementation details,  
 381 Section 6.2 validates the effectiveness of DML technique for improving generalization performance,  
 382 Section 6.3 verifies our central hypothesis, and Section 6.4 confirms our theoretical results.  
 383

384 

### 6.1 IMPLEMENTATION DETAILS

386 We use Procgen (Cobbe et al., 2019; 2020) as the experimental benchmark for testing generalization  
 387 performance. Procgen is a suite of 16 procedurally generated game-like environments designed to  
 388 benchmark both sample efficiency and generalization in reinforcement learning, and it has been  
 389 widely used to test the generalization performance of various reinforcement learning algorithms  
 390 (Wang et al., 2020; Raileanu & Fergus, 2021; Raileanu et al., 2021; Lyle et al., 2022; Rahman & Xue,  
 391 2023; Jesson & Jiang, 2024).

392 We employ the Proximal Policy Optimization (PPO) (Schulman et al., 2017; Cobbe et al., 2020) as  
 393 our baseline. Specifically, given a parameterized policy  $\pi_\theta$  ( $\theta$  represents the parameters), the objective  
 394 of  $\pi_\theta$  is to maximize

$$395 \quad J(\theta) = \mathbb{E}_{(o_t, a_t) \sim \pi_{\theta_{\text{old}}}} \left\{ \min \left[ r_t(\theta) \cdot \hat{A}(o_t, a_t), \text{clip}(r_t(\theta), 1 - \epsilon, 1 + \epsilon) \cdot \hat{A}(o_t, a_t) \right] \right\}, \quad (15)$$

398 where  $\hat{A}$  is the advantage estimate, and  $r_t(\theta) = \pi_\theta(a_t|o_t)/\pi_{\theta_{\text{old}}}(a_t|o_t)$  is the probability ratio, where  
 399  $\pi_{\theta_{\text{old}}}$  and  $\pi_\theta$  denote the old and current policies, respectively.

400 We randomly initialize two agents to interact with the environment and collect data separately. Similar  
 401 to the DML loss (4) used in supervised learning, we also introduce an additional KL divergence loss  
 402 term, which leads to

$$403 \quad \mathcal{L}_{\text{DML}} = \mathcal{L}_{\text{RL}} + \alpha \mathcal{L}_{\text{KL}}, \quad (16)$$

405 where  $\mathcal{L}_{\text{RL}}$  is the reinforcement learning loss and  $\mathcal{L}_{\text{KL}}$  is the KL divergence loss,  $\alpha$  is the weight.  
 406 And then we optimize the total loss of both agents, which is the average of their DML losses, as  
 407 shown in Algorithm 1, which we name Mutual Distillation Policy Optimization (MDPO).

408 **Algorithm 1** Mutual Distillation Policy Optimization (MDPO)

---

410 1: **Initialize:** Two agents  $\pi_1, \pi_2$ , PPO algorithm  $\mathcal{A}$ , KL divergence weight  $\alpha$   
 411 2: **while** training **do**  
 412 3:   **for**  $i = 1, 2$  **do**  
 413 4:     Collect training data:  $\mathcal{D}_i \sim \pi_i$   
 414 5:     Compute RL loss:  $\mathcal{L}_{\text{RL}}^{(i)} \leftarrow \mathcal{A}(\mathcal{D}_i)$   
 415 6:     Compute KL loss:  $\mathcal{L}_{\text{KL}}^{(i)} \leftarrow D_{\text{KL}}(\pi_{3-i} \parallel \pi_i)$   
 416 7:     Compute DML loss:  $\mathcal{L}_{\text{DML}}^{(i)} \leftarrow \mathcal{L}_{\text{RL}}^{(i)} + \alpha \mathcal{L}_{\text{KL}}^{(i)}$   
 417 8:   **end for**  
 418 9:   Compute total loss:  $\mathcal{L} \leftarrow \frac{1}{2} (\mathcal{L}_{\text{DML}}^{(1)} + \mathcal{L}_{\text{DML}}^{(2)})$   
 419 10:   Optimize  $\mathcal{L}$  using gradient descent algorithm  
 420 11: **end while**

---

422 Ultimately, we do not claim to achieve state-of-the-art (SOTA) performance, but rather provide  
 423 empirical evidence for the non-trivial insight that DML serves as an implicit regularization against  
 424 irrelevant features, leading to consistent improvements in generalization performance. We also  
 425 acknowledge the methodological similarities with prior work such as Zhao & Hospedales (2021);  
 426 despite that, we introduce *representation convergence* (Section 5.2), a novel insight with further  
 427 supported by strong theoretical analysis (Section 4), constituting our additional contributions.

429 

### 6.2 EMPIRICAL RESULTS

431 We compare the generalization performance of our MDPO against the PPO baseline on the Procgen  
 benchmark, under the hard-level settings (Cobbe et al., 2020), the results are illustrated in Figure 3. It

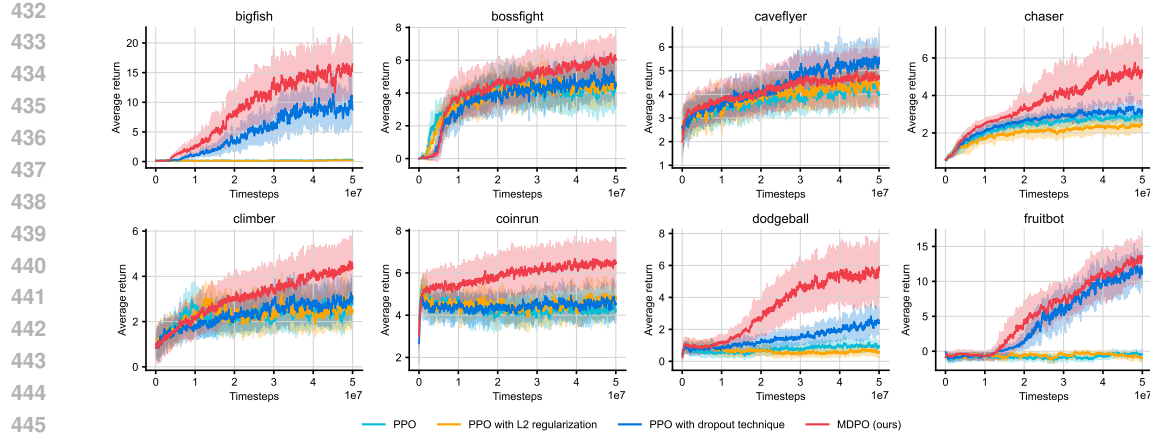


Figure 3: Generalization performance from 500 levels in Procgen benchmark with different methods. The mean and standard deviation are shown across 5 random seeds.

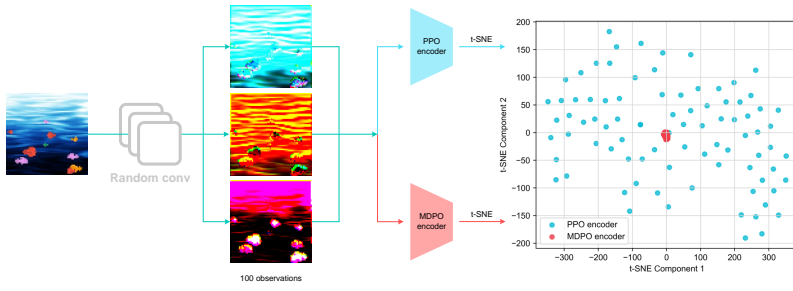


Figure 4: To test the robustness of the trained policy, we obfuscate the agent’s observations using convolutional layers randomly initialized with a standard Gaussian distribution.

can be observed that DML technique indeed leads to consistent improvements in generalization performance across all environments. Notably, for the bigfish, dodgeball, and fruitbot environments, we have observed significant improvements. Moreover, the full experimental results for all environments, including training and generalization performance, are provided in Appendix E.

A natural concern arises: how can we determine whether DML improves generalization performance by enhancing the policy robustness against irrelevant features, or simply due to the additional information sharing between these two agents during training (each agent receives additional information than it would from training alone)? To answer this question, we conducted robustness testing in Section 6.3 and added an ablation study in Section 6.4 to support our theory and hypothesis.

### 6.3 ROBUSTNESS TESTING

We design a novel approach to test policy robustness against irrelevant features. For a given frame, we generate *adversarial samples* using random CNNs initialized with a standard Gaussian distribution, as shown in Figure 4. Notably, the feature extraction of **MDPO** encoder is highly stable and focused (red points), whereas the features extracted by the original **PPO** encoder are significantly dispersed (blue points).

Moreover, we design a practical measure of  $\mathcal{R}$ -robustness defined in Definition 4.6. Specifically, for each environment, we run the trained policy (**PPO** and **MDPO**) in the environment for 100 steps and obtain observations

Algo\Env	caveflyer	chaser	climber	fruitbot
PPO	1.0000	1.0000	1.0000	1.0000
MDPO	0.9877	0.9982	0.8344	0.6973
Algo\Env	heist	jumper	leaper	plunder
PPO	0.9683	0.9699	1.0000	1.0000
MDPO	0.9142	0.9313	0.9423	0.9431

Table 1: A simple practical measure of  $\mathcal{R}$ -robustness defined in Definition 4.6.

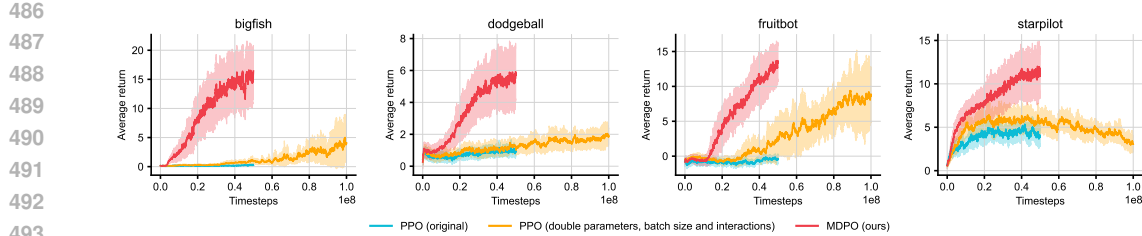


Figure 5: Generalization performance of **PPO baseline with double model size, batch size, and total number of interactions**, compared to original **PPO** and **MDPO** (for training results, see Figure 8).

$o_1, o_2, \dots, o_{100}$ . Then, for each  $o_i$  we use 100 random CNNs to simulate rendering function samples  $f_1^{(i)}, f_2^{(i)}, \dots, f_{100}^{(i)}$  and compute the TV divergence of the policy between the adversarial samples and the original observations, i.e.,  $D_{\text{TV}}(\pi_{\theta}(\cdot|o_i) \parallel \pi_{\theta}(\cdot|f_j^{(i)}(o_i)))$ , where  $i, j = 1, 2, \dots, 100$ . We then take the maximum of these values as a simple practical measure of  $\mathcal{R}$ -robustness:

$$\hat{\mathcal{R}} := \max_{i,j} D_{\text{TV}}(\pi_{\theta}(\cdot|o_i) \parallel \pi_{\theta}(\cdot|f_j^{(i)}(o_i))), \quad (17)$$

the results are shown in Table 1. We can see that **MDPO** achieves a significantly lower  $\hat{\mathcal{R}}$  than **PPO**, showing that DML effectively improves the policy robustness to irrelevant features, which serves as further strong evidence for our hypothesis.

#### 6.4 ABLATION STUDY

We design additional ablation experiments. Specifically, we *double* the model size, batch size, and total number of interactions for the PPO baseline, as shown in Figure 5. It can be seen that PPO baseline still fails to match the performance of **MDPO**, demonstrating that naively scaling up the **PPO** baseline does not lead to stable improvements in generalization performance.

Furthermore, we retrain a PPO *linear probe* on top of the *frozen* encoders of the trained **PPO** and **MDPO** policies, training for only 1M steps (2% of the original training steps), the final generalization performance during the last 10% steps is shown in Table 2. It can be seen that the PPO linear probe trained on the **MDPO** encoder achieves significantly better generalization performance, indicating that DML helps the policy learn better (more robust) representations. Moreover, we add a sensitivity analysis of the KL divergence weight  $\alpha$ , and the results are presented in Table 3.

## 7 CONCLUSION

In this paper, we provide a novel theoretical framework to explain the generalization problem in deep reinforcement learning. We further hypothesize that DML, as a form of implicit regularization, effectively prevents the policy from overfitting to irrelevant features. Strong empirical results support our central theory and hypothesis, demonstrating that our approach can improve the generalization performance of reinforcement learning systems by enhancing robustness against irrelevant features. Our work provides valuable insights and elegant solutions into the development of more adaptable and robust policies capable of generalizing across diverse environments.

540  
541  
ETHICS STATEMENT542  
543  
544  
All authors have read and adhere to the ICLR Code of Ethics. This paper does not involve studies  
with human subjects, dataset releases, potentially harmful insights, methodologies or applications,  
conflicts of interest, or concerns related to discrimination, bias, or fairness.545  
546  
547  
REPRODUCIBILITY STATEMENT548  
549  
550  
551  
We provide the full reproducible code in the supplementary materials, which is fully consistent with  
the hyperparameters listed in Appendix C. All theorems are fully proven in the appendix. Anyone  
can easily reproduce the results of our paper based on the provided code and hyperparameter settings.552  
553  
REFERENCES554  
555  
556  
Joshua Achiam, David Held, Aviv Tamar, and Pieter Abbeel. Constrained policy optimization. In  
*International conference on machine learning*, pp. 22–31. PMLR, 2017.557  
558  
559  
Sara L Bengtsson, John-Dylan Haynes, Katsuyuki Sakai, Mark J Buckley, and Richard E Passingham.  
The representation of abstract task rules in the human prefrontal cortex. *Cerebral Cortex*, 19(8):  
1929–1936, 2009.560  
561  
562  
Karl Cobbe, Oleg Klimov, Chris Hesse, Taehoon Kim, and John Schulman. Quantifying generalization  
in reinforcement learning. In *International conference on machine learning*, pp. 1282–1289. PMLR,  
2019.563  
564  
565  
Karl Cobbe, Chris Hesse, Jacob Hilton, and John Schulman. Leveraging procedural generation  
to benchmark reinforcement learning. In *International conference on machine learning*, pp.  
2048–2056. PMLR, 2020.566  
567  
568  
Karl W Cobbe, Jacob Hilton, Oleg Klimov, and John Schulman. Phasic policy gradient. In *International  
Conference on Machine Learning*, pp. 2020–2027. PMLR, 2021.569  
570  
571  
Lucas Deckers, Benjamin Vandersmissen, Ing Jyh Tsang, Werner Van Leekwijck, and Steven Latré.  
Twin network augmentation: A novel training strategy for improved spiking neural networks and  
efficient weight quantization. *arXiv preprint arXiv:2409.15849*, 2024.572  
573  
574  
Iroise Dumontheil. Development of abstract thinking during childhood and adolescence: The role of  
rostrolateral prefrontal cortex. *Developmental cognitive neuroscience*, 10:57–76, 2014.575  
576  
577  
Jesse Farebrother, Marlos C Machado, and Michael Bowling. Generalization and regularization in  
dqn. *arXiv preprint arXiv:1810.00123*, 2018.578  
579  
580  
Yaozhong Gan, Renye Yan, Xiaoyang Tan, Zhe Wu, and Junliang Xing. Transductive off-policy  
proximal policy optimization. *arXiv preprint arXiv:2406.03894*, 2024.581  
582  
Ian J Goodfellow, Jonathon Shlens, and Christian Szegedy. Explaining and harnessing adversarial  
examples. *arXiv preprint arXiv:1412.6572*, 2014.583  
584  
585  
Jake Grigsby and Yanjun Qi. Measuring visual generalization in continuous control from pixels.  
*arXiv preprint arXiv:2010.06740*, 2020.586  
587  
588  
Shengyi Huang, Rousslan Fernand Julien Dossa, Chang Ye, Jeff Braga, Dipam Chakraborty, Kinal  
Mehta, and JoĂGo GM AraĂjo. Cleanrl: High-quality single-file implementations of deep  
reinforcement learning algorithms. *Journal of Machine Learning Research*, 23(274):1–18, 2022.589  
590  
591  
Maximilian Igl, Kamil Ciosek, Yingzhen Li, Sebastian Tschiatschek, Cheng Zhang, Sam Devlin,  
and Katja Hofmann. Generalization in reinforcement learning with selective noise injection and  
information bottleneck. *Advances in neural information processing systems*, 32, 2019.592  
593  
Andrew Jesson and Yiding Jiang. Improving generalization on the procgen benchmark with simple  
architectural changes and scale. *arXiv preprint arXiv:2410.10905*, 2024.

594 Yiding Jiang, J Zico Kolter, and Roberta Raileanu. On the importance of exploration for generalization  
 595 in reinforcement learning. *Advances in Neural Information Processing Systems*, 36:12951–12986,  
 596 2023.

597

598 Niels Justesen, Ruben Rodriguez Torrado, Philip Bontrager, Ahmed Khalifa, Julian Togelius, and  
 599 Sebastian Risi. Illuminating generalization in deep reinforcement learning through procedural  
 600 level generation. *arXiv preprint arXiv:1806.10729*, 2018.

601 Sham Kakade and John Langford. Approximately optimal approximate reinforcement learning. In  
 602 *Proceedings of the nineteenth international conference on machine learning*, pp. 267–274, 2002.  
 603

604 Nathan Kallus and Angela Zhou. Confounding-robust policy evaluation in infinite-horizon reinforce-  
 605 ment learning. *Advances in neural information processing systems*, 33:22293–22304, 2020.

606

607 Robert Kirk, Amy Zhang, Edward Grefenstette, and Tim Rocktäschel. A survey of zero-shot  
 608 generalisation in deep reinforcement learning. *Journal of Artificial Intelligence Research*, 76:  
 609 201–264, 2023.

610 Kwei-Herng Lai, Daochen Zha, Yuening Li, and Xia Hu. Dual policy distillation. *arXiv preprint*  
 611 *arXiv:2006.04061*, 2020.

612

613 Misha Laskin, Kimin Lee, Adam Stooke, Lerrel Pinto, Pieter Abbeel, and Aravind Srinivas. Rein-  
 614 forcement learning with augmented data. *Advances in neural information processing systems*, 33:  
 615 19884–19895, 2020.

616 Kimin Lee, Kibok Lee, Jinwoo Shin, and Honglak Lee. Network randomization: A simple technique  
 617 for generalization in deep reinforcement learning. *arXiv preprint arXiv:1910.05396*, 2019.

618

619 Clare Lyle, Mark Rowland, Will Dabney, Marta Kwiatkowska, and Yarin Gal. Learning dynamics and  
 620 generalization in deep reinforcement learning. In *International Conference on Machine Learning*,  
 621 pp. 14560–14581. PMLR, 2022.

622

623 Guozheng Ma, Zhen Wang, Zhecheng Yuan, Xueqian Wang, Bo Yuan, and Dacheng Tao. A  
 624 comprehensive survey of data augmentation in visual reinforcement learning. *arXiv preprint*  
*arXiv:2210.04561*, 2022.

625

626 Bogdan Mazoure, Ahmed M Ahmed, Patrick MacAlpine, R Devon Hjelm, and Andrey Kolobov.  
 627 Cross-trajectory representation learning for zero-shot generalization in rl. *arXiv preprint*  
*arXiv:2106.02193*, 2021.

629

630 Bhairav Mehta, Manfred Diaz, Florian Golemo, Christopher J Pal, and Liam Paull. Active domain  
 631 randomization. In *Conference on Robot Learning*, pp. 1162–1176. PMLR, 2020.

632

633 Seungyong Moon, JunYeong Lee, and Hyun Oh Song. Rethinking value function learning for  
 634 generalization in reinforcement learning. *Advances in Neural Information Processing Systems*, 35:  
 34846–34858, 2022.

635

636 A Tuan Nguyen, Toan Tran, Yarin Gal, and Atilim Gunes Baydin. Domain invariant representation  
 637 learning with domain density transformations. *Advances in Neural Information Processing Systems*,  
 638 34:5264–5275, 2021.

639

640 Charles Packer, Katelyn Gao, Jernej Kos, Philipp Krähenbühl, Vladlen Koltun, and Dawn Song.  
 641 Assessing generalization in deep reinforcement learning. *arXiv preprint arXiv:1810.12282*, 2018.

641

642 Hyun-Jae Pi, Balázs Hangya, Duda Kvitsiani, Joshua I Sanders, Z Josh Huang, and Adam Kepecs.  
 643 Cortical interneurons that specialize in disinhibitory control. *Nature*, 503(7477):521–524, 2013.

644

645 Md Masudur Rahman and Yexiang Xue. Adversarial style transfer for robust policy optimization in  
 646 deep reinforcement learning. *arXiv preprint arXiv:2308.15550*, 2023.

646

647 Roberta Raileanu and Rob Fergus. Decoupling value and policy for generalization in reinforcement  
 648 learning. In *International Conference on Machine Learning*, pp. 8787–8798. PMLR, 2021.

648 Roberta Raileanu, Maxwell Goldstein, Denis Yarats, Ilya Kostrikov, and Rob Fergus. Automatic  
 649 data augmentation for generalization in reinforcement learning. *Advances in Neural Information  
 650 Processing Systems*, 34:5402–5415, 2021.

651 Aravind Rajeswaran, Kendall Lowrey, Emanuel V Todorov, and Sham M Kakade. Towards general-  
 652 ization and simplicity in continuous control. *Advances in neural information processing systems*,  
 653 30, 2017.

654 John Schulman, Sergey Levine, Pieter Abbeel, Michael Jordan, and Philipp Moritz. Trust region  
 655 policy optimization. In *International conference on machine learning*, pp. 1889–1897. PMLR,  
 656 2015.

657 John Schulman, Filip Wolski, Prafulla Dhariwal, Alec Radford, and Oleg Klimov. Proximal policy  
 658 optimization algorithms. *arXiv preprint arXiv:1707.06347*, 2017.

659 Connor Shorten and Taghi M Khoshgoftaar. A survey on image data augmentation for deep learning.  
 660 *Journal of big data*, 6(1):1–48, 2019.

661 Reda Bahi Slaoui, William R Clements, Jakob N Foerster, and Sébastien Toth. Robust visual domain  
 662 randomization for reinforcement learning. *arXiv preprint arXiv:1910.10537*, 2019.

663 Richard D Smallwood and Edward J Sondik. The optimal control of partially observable markov  
 664 processes over a finite horizon. *Operations research*, 21(5):1071–1088, 1973.

665 Xingyou Song, Yiding Jiang, Stephen Tu, Yilun Du, and Behnam Neyshabur. Observational overfitting  
 666 in reinforcement learning. *arXiv preprint arXiv:1912.02975*, 2019.

667 Nitish Srivastava, Geoffrey Hinton, Alex Krizhevsky, Ilya Sutskever, and Ruslan Salakhutdinov.  
 668 Dropout: a simple way to prevent neural networks from overfitting. *The journal of machine  
 669 learning research*, 15(1):1929–1958, 2014.

670 Miguel Suau, Matthijs TJ Spaan, and Frans A Oliehoek. Bad habits: Policy confounding and  
 671 out-of-trajectory generalization in rl. *arXiv preprint arXiv:2306.02419*, 2023.

672 Josh Tobin, Rachel Fong, Alex Ray, Jonas Schneider, Wojciech Zaremba, and Pieter Abbeel. Domain  
 673 randomization for transferring deep neural networks from simulation to the real world. In *2017  
 674 IEEE/RSJ international conference on intelligent robots and systems (IROS)*, pp. 23–30. IEEE,  
 675 2017.

676 Benjamin Vandersmissen, Lucas Deckers, and Jose Oramas. Improving neural network accuracy by  
 677 concurrently training with a twin network. In *The Thirteenth International Conference on Learning  
 678 Representations*.

679 Kaixin Wang, Bingyi Kang, Jie Shao, and Jiashi Feng. Improving generalization in reinforcement  
 680 learning with mixture regularization. *Advances in Neural Information Processing Systems*, 33:  
 681 7968–7978, 2020.

682 Max Weltevreden, Caroline Horsch, Matthijs TJ Spaan, and Wendelin Böhmer. Exploration im-  
 683 plies data augmentation: Reachability and generalisation in contextual mdps. *arXiv preprint  
 684 arXiv:2410.03565*, 2024.

685 Max Weltevreden, Moritz A Zanger, Matthijs TJ Spaan, and Wendelin Böhmer. How ensembles of dis-  
 686 tillied policies improve generalisation in reinforcement learning. *arXiv preprint arXiv:2505.16581*,  
 687 2025.

688 Zhengpeng Xie, Qiang Zhang, Fan Yang, Marco Hutter, and Renjing Xu. Simple policy optimization.  
 689 In *Forty-second International Conference on Machine Learning*, 2025.

690 Xiaohan Xu, Ming Li, Chongyang Tao, Tao Shen, Reynold Cheng, Jinyang Li, Can Xu, Dacheng Tao,  
 691 and Tianyi Zhou. A survey on knowledge distillation of large language models. *arXiv preprint  
 692 arXiv:2402.13116*, 2024.

693 Denis Yarats, Ilya Kostrikov, and Rob Fergus. Image augmentation is all you need: Regularizing  
 694 deep reinforcement learning from pixels. In *International conference on learning representations*,  
 695 2021.

702 Sing-Yuan Yeh, Fu-Chieh Chang, Chang-Wei Yueh, Pei-Yuan Wu, Alberto Bernacchia, and Sattar  
 703 Vakili. Sample complexity of kernel-based q-learning. In *International Conference on Artificial  
 704 Intelligence and Statistics*, pp. 453–469. PMLR, 2023.

705 Zhecheng Yuan, Sizhe Yang, Pu Hua, Can Chang, Kaizhe Hu, and Huazhe Xu. Rl-vigen: A  
 706 reinforcement learning benchmark for visual generalization. *Advances in Neural Information  
 707 Processing Systems*, 36:6720–6747, 2023.

708 Xiangyu Yue, Yang Zhang, Sicheng Zhao, Alberto Sangiovanni-Vincentelli, Kurt Keutzer, and  
 709 Boqing Gong. Domain randomization and pyramid consistency: Simulation-to-real generalization  
 710 without accessing target domain data. In *Proceedings of the IEEE/CVF international conference  
 711 on computer vision*, pp. 2100–2110, 2019.

712 Amy Zhang, Rowan McAllister, Roberto Calandra, Yarin Gal, and Sergey Levine. Learning  
 713 invariant representations for reinforcement learning without reconstruction. *arXiv preprint  
 714 arXiv:2006.10742*, 2020.

715 Chiyuan Zhang, Oriol Vinyals, Remi Munos, and Samy Bengio. A study on overfitting in deep  
 716 reinforcement learning. *arXiv preprint arXiv:1804.06893*, 2018a.

717 Hanping Zhang and Yuhong Guo. Generalization of reinforcement learning with policy-aware  
 718 adversarial data augmentation. *arXiv preprint arXiv:2106.15587*, 2021.

719 Ying Zhang, Tao Xiang, Timothy M Hospedales, and Huchuan Lu. Deep mutual learning. In  
 720 *Proceedings of the IEEE conference on computer vision and pattern recognition*, pp. 4320–4328,  
 721 2018b.

722 Chenyang Zhao and Timothy Hospedales. Robust domain randomised reinforcement learning through  
 723 peer-to-peer distillation. In *Asian Conference on Machine Learning*, pp. 1237–1252. PMLR, 2021.

724 Zifeng Zhuang, Kun Lei, Jinxin Liu, Donglin Wang, and Yilang Guo. Behavior proximal policy  
 725 optimization. *arXiv preprint arXiv:2302.11312*, 2023.

726

727

728

729

730

731

732

733

734

735

736

737

738

739

740

741

742

743

744

745

746

747

748

749

750

751

752

753

754

755

756 **A LLM USAGE**  
757758 In this work, large language models (LLMs) were used to assist in refining and polishing the writing.  
759760 **B LIMITATIONS**  
761762 While our method demonstrates that mutual distillation improves robustness and generalization, it  
763 inevitably introduces additional computational costs. Specifically, MDPO requires *twice* the number  
764 of trainable parameters and roughly twice the environment interaction steps compared to a single-  
765 policy baseline. Consequently, the method may be less practical in settings with limited computational  
766 resources or when sample efficiency is critical. Addressing these efficiency concerns, such as via  
767 parameter sharing or selective distillation, is an interesting direction for future work.  
768769 **C HYPERPARAMETERS**  
770771 Table 4 shows the detailed hyperparameter settings in our code, with the main hyperparameters  
772 consistent with the hard-level settings in [Cobbe et al. \(2020\)](#), except that we train for 50M steps instead  
773 of 200M. We train the policy on the initial 500 levels and then test its generalization performance  
774 across the full distribution of levels.  
775776 Table 4: Detailed hyperparameters in Procgen.  
777

Hyperparameter\Algorithm	PPO ( <a href="#">Schulman et al., 2017</a> )	MDPO (ours)
Number of workers	64	64
Horizon	256	256
Learning rate	0.0005	0.0005
Learning rate decay	No	No
Optimizer	Adam	Adam
Total interaction steps	50M	50M
Update epochs	3	3
Mini-batches	8	8
Batch size	16384	16384
Mini-batch size	2048	2048
Discount factor $\gamma$	0.999	0.999
GAE parameter $\lambda$	0.95	0.95
Value loss coefficient $c_1$	0.5	0.5
Entropy loss coefficient $c_2$	0.01	0.01
Clipping parameter $\epsilon$	0.2	0.2
KL divergence weight $\alpha$	-	1.0

790  
791  
792  
793  
794  
795  
796  
797  
798  
799  
800  
801  
802  
803  
804  
805  
806  
807  
808  
809

## 810 D THE REPRESENTATION CONVERGENCE PHENOMENON

812 To further demonstrate that mutual distillation indeed promotes representation convergence, we  
 813 conducted the following experiment: we compared the *Centered Kernel Alignment* (CKA) of two  
 814 agents in MDPO on the same batch of adversarial examples at different training stages, under different  
 815 KL divergence weight  $\alpha$ , the results are shown in the Table 5 below:

817 Table 5: CKA of two MDPO policies under different  $\alpha$ .

Algo\Training stage	0%	25%	50%	75%	100%
MDPO ( $\alpha = 1.0$ )	0.649	0.769	0.797	0.850	0.867
MDPO ( $\alpha = 0.0$ )	0.649	0.185	0.131	0.146	0.004

822 It is evident that after mutual distillation ( $\alpha = 1.0$ ), the two agents learned more robust representations,  
 823 as their representations of the same batch of adversarial examples became increasingly similar. In  
 824 contrast, when the distillation weight  $\alpha = 0.0$ , their representations diverge over time. We further  
 825 evaluated the *cosine similarity* of the representations of adversarial examples encoded by PPO and  
 826 MDPO across four environments, as shown in the Table 6.

827 Table 6: Cosine similarity of the representations.

Algo\Env	coinrun	dodgeball	fruitbot	starpilot
PPO encoder	0.301	-0.006	0.180	0.027
MDPO encoder	<b>0.781</b>	<b>0.585</b>	<b>0.547</b>	<b>0.718</b>

833 We can see that MDPO achieves significantly higher cosine similarity for the adversarial samples,  
 834 showing that MDPO has learned more robust representations with respect to irrelevant features.

864  
865  
866  
867  
868  
869  
870  
871  
872  
873  
874  
875  
876  
877  
878  
879  
880  
881  
882  
883  
884  
885  
886  
887  
888  
889  
890  
891  
892  
893  
894  
895  
896  
897  
898  
899  
900  
901  
902  
903  
904  
905  
906  
907  
908  
909  
910  
911  
912  
913  
914  
915  
916  
917  
E MORE RESULTS

## E.1 FULL RESULTS

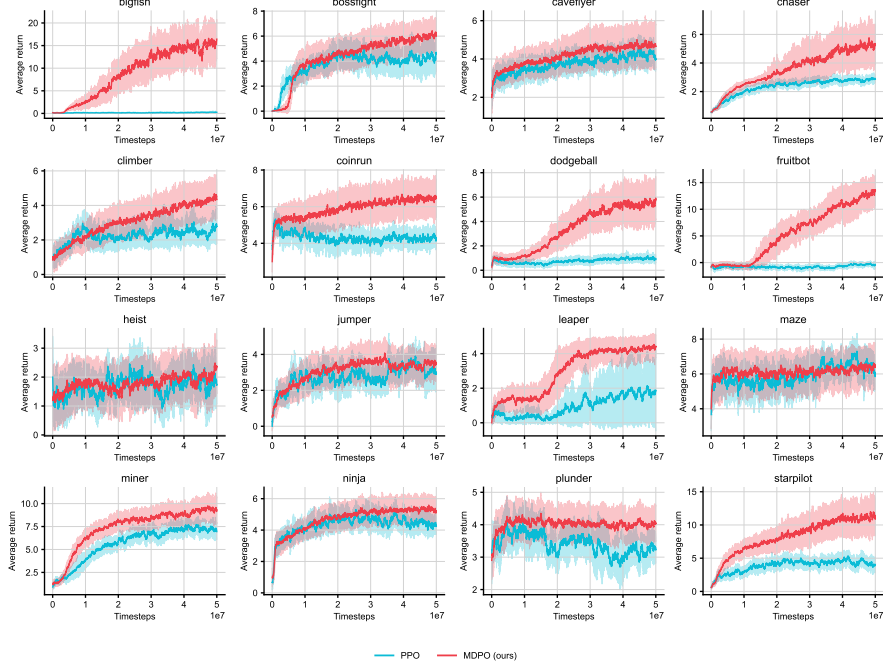


Figure 6: Generalization performance of PPO and MDPO from 500 levels in each environment.

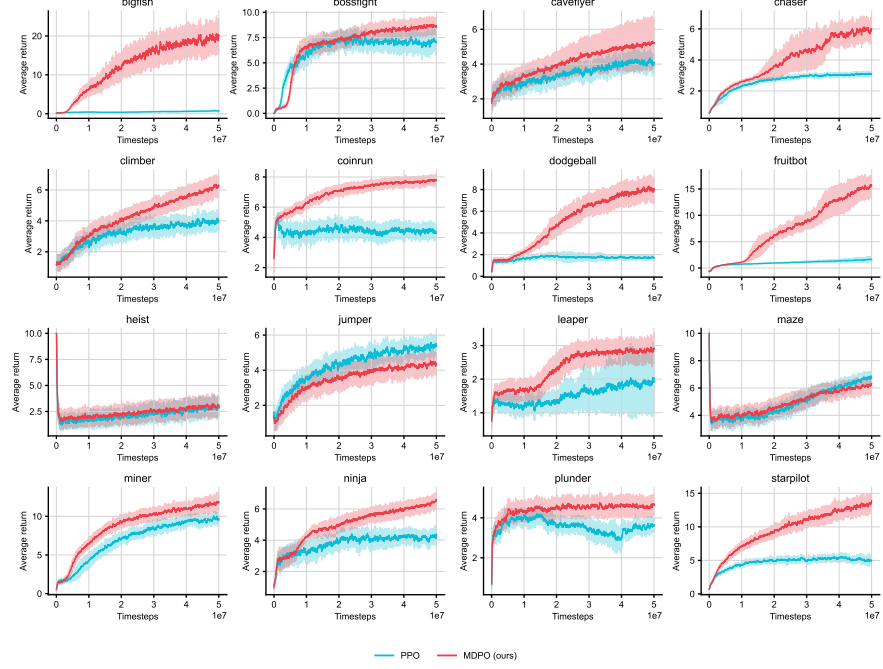
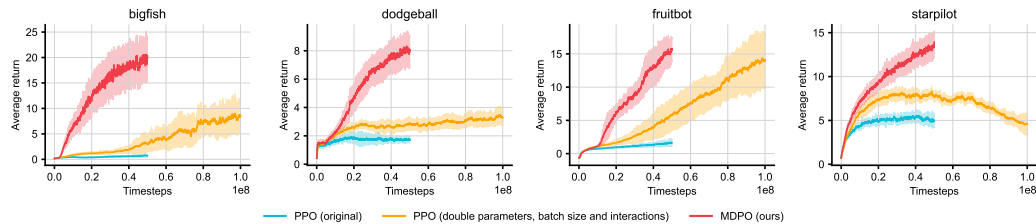
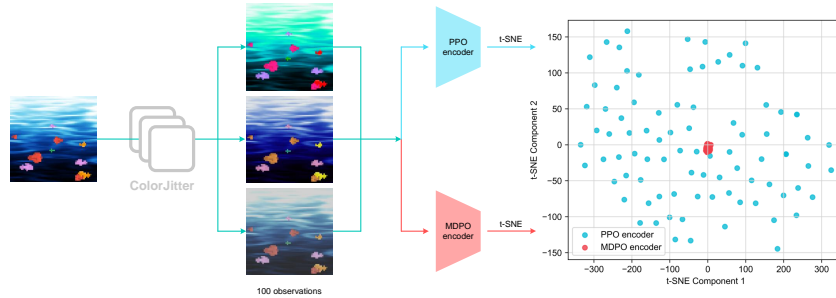
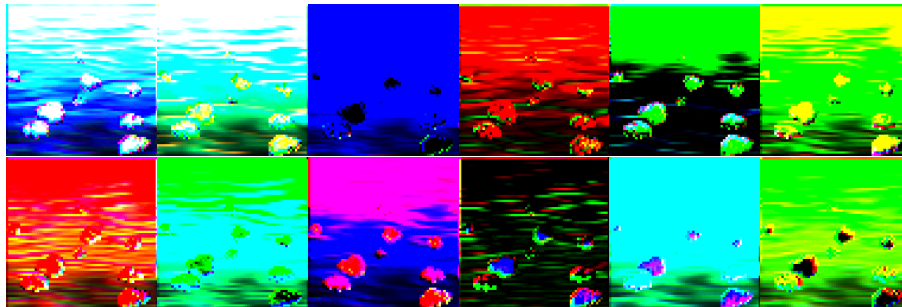
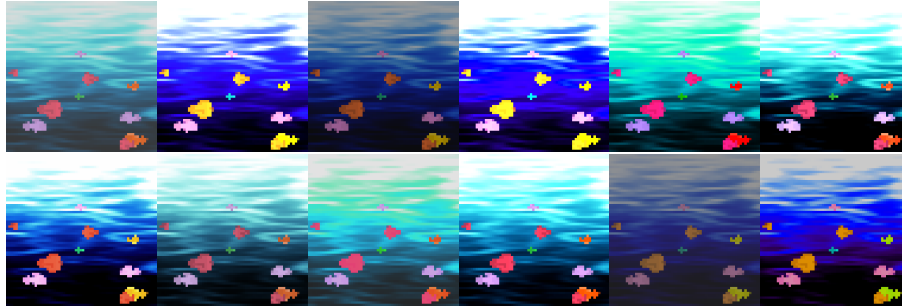


Figure 7: Training performance of PPO and MDPO from 500 levels in each environment.

918 E.2 MORE ABLATION RESULTS  
919920 Here, we additionally present the training curves from the Ablation Study (Section 6.4), as shown in  
921 Figure 8.  
922931 Figure 8: Training performance of **PPO baseline with double model size, batch size, and total number**  
932 **of interactions**, compared to original **PPO** and **MDPO**.  
933934 Interestingly, although the **scaled-up PPO** nearly matches **MDPO** in training performance during  
935 the final stage of training in the fruitbot environment, there remains a substantial gap in their  
936 generalization performance (as shown in Figure 5). This provides further strong evidence that DML  
937 effectively enhances the policy robustness to irrelevant features, as **MDPO** achieves significantly  
938 better generalization performance despite comparable training performance.  
939  
940  
941  
942  
943  
944  
945  
946  
947  
948  
949  
950  
951  
952  
953  
954  
955  
956  
957  
958  
959  
960  
961  
962  
963  
964  
965  
966  
967  
968  
969  
970  
971

972 E.3 ADDITIONAL VISUALIZATIONS  
973974 We also generate adversarial samples by adjusting the brightness, contrast, saturation, and hue of the  
975 images, and test the robustness of the **PPO** encoder and our **MDPO** encoder, as shown in Figure 9.  
976977 Figure 9: The robustness of PPO and MDPO to brightness, contrast, saturation, and hue.  
978  
979980 We can see that the **MDPO** policy has also learned robustness representations to these irrelevant  
981 factors, while the **PPO** policy remains sensitive to them. Additionally, we present adversarial samples  
982 generated by random CNNs, as shown in Figure 10, as well as those generated by randomly adjusting  
983 brightness, contrast, saturation, and hue, as can be seen from Figure 11.  
984985 Figure 10: Adversarial samples generated by random CNNs.  
986  
987988 Figure 11: Adversarial samples generated by different brightness, contrast, saturation, and hue.  
989  
990

1026 **F PROOFS**

1028 Let's start with some useful lemmas.

1029 **Lemma F.1** (Performance difference). *Let  $\mu_f(\cdot|s_t) = \pi(\cdot|f(s_t))$  and  $\tilde{\mu}_f(\cdot|s_t) = \tilde{\pi}(\cdot|f(s_t))$ ,  
1030 define training and generalization performance as*

$$1032 \eta(\pi) = \frac{1}{1-\gamma} \mathbb{E}_{\substack{f \sim p_{\text{train}}(\cdot) \\ s \sim d^{\mu_f}(\cdot) \\ a \sim \mu_f(\cdot|s)}} [r(s, a)], \quad \zeta(\pi) = \frac{1}{1-\gamma} \mathbb{E}_{\substack{f \sim p(\cdot) \\ s \sim d^{\tilde{\mu}_f}(\cdot) \\ a \sim \tilde{\mu}_f(\cdot|s)}} [r(s, a)]. \quad (18)$$

1035 Then the differences in training and generalization performance can be expressed as

$$1037 \eta(\tilde{\pi}) - \eta(\pi) = \frac{1}{1-\gamma} \mathbb{E}_{\substack{f \sim p_{\text{train}}(\cdot) \\ s \sim d^{\mu_f}(\cdot) \\ a \sim \tilde{\mu}_f(\cdot|s)}} [A^{\mu_f}(s, a)], \quad \zeta(\tilde{\pi}) - \zeta(\pi) = \frac{1}{1-\gamma} \mathbb{E}_{\substack{f \sim p(\cdot) \\ s \sim d^{\tilde{\mu}_f}(\cdot) \\ a \sim \tilde{\mu}_f(\cdot|s)}} [A^{\mu_f}(s, a)]. \quad (19)$$

1041 *Proof.* This result can be directly derived from Kakade & Langford (2002).  $\square$

1044 **Lemma F.2.** *The divergence between two normalized discounted visitation distribution,  $\|d^{\tilde{\mu}} - d^{\mu}\|_1$ , is bounded by an average divergence of  $\tilde{\mu}$  and  $\mu$ :*

$$1046 \|d^{\tilde{\mu}} - d^{\mu}\|_1 \leq \frac{\gamma}{1-\gamma} \mathbb{E}_{s \sim d^{\mu}(\cdot)} [\|\tilde{\mu} - \mu\|_1] = \frac{2\gamma}{1-\gamma} \mathbb{E}_{s \sim d^{\mu}(\cdot)} [D_{\text{TV}}(\tilde{\mu}\|\mu)[s]], \quad (20)$$

1049 where  $D_{\text{TV}}(\tilde{\mu}\|\mu)[s] = \frac{1}{2} \sum_{a \in \mathcal{A}} |\tilde{\mu}(a|s) - \mu(a|s)|$  represents the Total Variation (TV) distance.

1051 *Proof.* See Achiam et al. (2017).  $\square$

1053 **Lemma F.3.** *Given any state  $s \in \mathcal{S}$ , any two policies  $\tilde{\mu}$  and  $\mu$ , the average advantage,  $\mathbb{E}_{a \sim \tilde{\mu}(\cdot|s)} [A^{\mu}(s, a)]$ , is bounded by*

$$1055 \left| \mathbb{E}_{a \sim \tilde{\mu}(\cdot|s)} [A^{\mu}(s, a)] \right| \leq 2D_{\text{TV}}(\tilde{\mu}\|\mu)[s] \cdot \max_a |A^{\mu}(s, a)|. \quad (21)$$

1058 *Proof.* Note that

$$1060 \mathbb{E}_{a \sim \mu(\cdot|s)} [A^{\mu}(s, a)] = \mathbb{E}_{a \sim \mu(\cdot|s)} [Q^{\mu}(s, a) - V^{\mu}(s)] \\ 1061 = \mathbb{E}_{a \sim \mu(\cdot|s)} [Q^{\mu}(s, a)] - V^{\mu}(s) \\ 1062 = V^{\mu}(s) - V^{\mu}(s) \\ 1063 = 0,$$

1064 thus,

$$1066 \left| \mathbb{E}_{a \sim \tilde{\mu}(\cdot|s)} [A^{\mu}(s, a)] \right| = \left| \mathbb{E}_{a \sim \tilde{\mu}(\cdot|s)} [A^{\mu}(s, a)] - \mathbb{E}_{a \sim \mu(\cdot|s)} [A^{\mu}(s, a)] \right| \\ 1067 \leq \|\tilde{\mu} - \mu\|_1 \cdot \|A^{\mu}(s, a)\|_{\infty} \\ 1068 = 2D_{\text{TV}}(\tilde{\mu}\|\mu)[s] \cdot \max_a |A^{\mu}(s, a)|. \quad (23)$$

1070 This is a widely used trick (Schulman et al., 2015; Zhuang et al., 2023; Gan et al., 2024).  $\square$

1072 In addition, using the above lemmas, the following corollary can be obtained, which will be repeatedly  
1073 used in our proof.

1074 **Corollary F.4.** *Given any two policies,  $\tilde{\mu}$  and  $\mu$ , the following bound holds:*

$$1076 \left| \mathbb{E}_{\substack{s \sim d^{\tilde{\mu}}(\cdot) \\ a \sim \tilde{\mu}(\cdot|s)}} [A^{\mu}(s, a)] - \mathbb{E}_{\substack{s \sim d^{\mu}(\cdot) \\ a \sim \tilde{\mu}(\cdot|s)}} [A^{\mu}(s, a)] \right| \leq \frac{2\epsilon\gamma}{1-\gamma} \mathbb{E}_{s \sim d^{\mu}(\cdot)} [D_{\text{TV}}(\tilde{\mu}\|\mu)[s]], \quad (24)$$

1080 where  $\epsilon = \max_s |\mathbb{E}_{a \sim \tilde{\mu}(\cdot|s)} [A^\mu(s, a)]|$ .  
 1081

1082 *Proof.* We rewrite the expectation as  
 1083

$$1084 \left| \mathbb{E}_{\substack{s \sim d^\mu(\cdot) \\ a \sim \tilde{\mu}(\cdot|s)}} [A^\mu(s, a)] - \mathbb{E}_{\substack{s \sim d^\mu(\cdot) \\ a \sim \tilde{\mu}(\cdot|s)}} [A^\mu(s, a)] \right| = \left| \mathbb{E}_{s \sim d^\mu(\cdot)} \left\{ \mathbb{E}_{a \sim \tilde{\mu}(\cdot|s)} [A^\mu(s, a)] \right\} - \mathbb{E}_{s \sim d^\mu(\cdot)} \left\{ \mathbb{E}_{a \sim \tilde{\mu}(\cdot|s)} [A^\mu(s, a)] \right\} \right|, \\ 1085 \quad 1086 \quad 1087 \quad 1088 \quad 1089 \quad 1090 \quad 1091 \quad 1092 \quad 1093 \quad 1094 \quad 1095 \quad 1096 \quad 1097 \quad 1098 \quad 1099 \quad 1100 \quad 1101 \quad 1102 \quad 1103 \quad 1104 \quad 1105 \quad 1106 \quad 1107 \quad 1108 \quad 1109 \quad 1110 \quad 1111 \quad 1112 \quad 1113 \quad 1114 \quad 1115 \quad 1116 \quad 1117 \quad 1118 \quad 1119 \quad 1120 \quad 1121 \quad 1122 \quad 1123 \quad 1124 \quad 1125 \quad 1126 \quad 1127 \quad 1128 \quad 1129 \quad 1130 \quad 1131 \quad 1132 \quad 1133$$

$$(25)$$

where the expectation  $\mathbb{E}_{a \sim \tilde{\mu}(\cdot|s)} [A^\mu(s, a)]$  is a function of  $s$ , then

$$\left| \mathbb{E}_{s \sim d^\mu(\cdot)} \left\{ \mathbb{E}_{a \sim \tilde{\mu}(\cdot|s)} [A^\mu(s, a)] \right\} - \mathbb{E}_{s \sim d^\mu(\cdot)} \left\{ \mathbb{E}_{a \sim \tilde{\mu}(\cdot|s)} [A^\mu(s, a)] \right\} \right| \leq \|d^\mu - d^\mu\|_1 \cdot \left\| \mathbb{E}_{a \sim \tilde{\mu}(\cdot|s)} [A^\mu(s, a)] \right\|_\infty. \quad (26)$$

Next, according to Lemma F.2, we have

$$\|d^\mu - d^\mu\|_1 \cdot \left\| \mathbb{E}_{a \sim \tilde{\mu}(\cdot|s)} [A^\mu(s, a)] \right\|_\infty = \|d^\mu - d^\mu\|_1 \cdot \epsilon \leq \frac{2\epsilon\gamma}{1-\gamma} \mathbb{E}_{s \sim d^\mu(\cdot)} [D_{\text{TV}}(\tilde{\mu} \parallel \mu)[s]], \quad (27)$$

concluding the proof.  $\square$

## F.1 PROOF OF LEMMA 4.2

**Lemma 4.2.** For any given policy  $\pi$ , define its underlying policy as  $\mu_f(\cdot|s_t) = \pi(\cdot|f(s_t))$ , then

$$\eta(\pi) = \frac{1}{1-\gamma} \mathbb{E}_{\substack{f \sim p_{\text{train}}(\cdot) \\ s \sim d^{\mu_f}(\cdot) \\ a \sim \mu_f(\cdot|s)}} [r(s, a)], \quad \zeta(\pi) = \frac{1}{1-\gamma} \mathbb{E}_{\substack{f \sim p(\cdot) \\ s \sim d^{\mu_f}(\cdot) \\ a \sim \mu_f(\cdot|s)}} [r(s, a)]. \quad (28)$$

According to the definition of training and generalization performance in (3), we have

$$\eta(\pi) = \mathbb{E}_{f \sim p_{\text{train}}(\cdot), \tau_f \sim \pi} \left[ \sum_{t=0}^{\infty} \gamma^t r_f(o_t^f, a_t) \right], \quad \zeta(\pi) = \mathbb{E}_{f \sim p(\cdot), \tau_f \sim \pi} \left[ \sum_{t=0}^{\infty} \gamma^t r_f(o_t^f, a_t) \right]. \quad (29)$$

To prove Lemma 4.2, we only need to show that for any given  $f \in \mathcal{F}$ , the following equation holds:

$$\frac{1}{1-\gamma} \mathbb{E}_{\substack{s \sim d^{\mu_f}(\cdot) \\ a \sim \mu_f(\cdot|s)}} [r(s, a)] = \mathbb{E}_{\tau_f \sim \pi} \left[ \sum_{t=0}^{\infty} \gamma^t r_f(o_t^f, a_t) \right]. \quad (30)$$

According to the definition of the normalized discounted visitation distribution  $d^\mu(s) = (1 - \gamma) \sum_{t=0}^{\infty} \gamma^t \mathbb{P}(s_t = s | \mu)$ , we have

$$\begin{aligned} \frac{1}{1-\gamma} \mathbb{E}_{\substack{s \sim d^{\mu_f}(\cdot) \\ a \sim \mu_f(\cdot|s)}} [r(s, a)] &= \frac{1}{1-\gamma} \sum_{s \in \mathcal{S}} (1-\gamma) \sum_{t=0}^{\infty} \gamma^t \mathbb{P}(s_t = s | \mu_f) \sum_{a \in \mathcal{A}} \mu_f(a|s) \cdot r(s, a) \\ &= \sum_{t=0}^{\infty} \sum_{s \in \mathcal{S}} \mathbb{P}(s_t = s | \mu_f) \sum_{a \in \mathcal{A}} \mu_f(a|s) \cdot \gamma^t r(s, a) \end{aligned} \quad (31)$$

Next, according to Assumption 3.2, we have

$$\begin{aligned} \frac{1}{1-\gamma} \mathbb{E}_{\substack{s \sim d^{\mu_f}(\cdot) \\ a \sim \mu_f(\cdot|s)}} [r(s, a)] &= \sum_{t=0}^{\infty} \sum_{s \in \mathcal{S}} \mathbb{P}(s_t = s | \mu_f) \sum_{a \in \mathcal{A}} \mu_f(a|s) \cdot \gamma^t r(s, a) \\ &= \sum_{t=0}^{\infty} \sum_{s \in \mathcal{S}} \mathbb{P}(f(s_t) = f(s) | \mu_f) \sum_{a \in \mathcal{A}} \pi(a|f(s)) \cdot \gamma^t r_f(f(s), a) \\ &\stackrel{f(s)=o^f, f(s_t)=o_t^f}{=} \sum_{t=0}^{\infty} \sum_{o^f \in \mathcal{O}_f} \mathbb{P}(o_t^f = o^f | \pi) \sum_{a \in \mathcal{A}} \pi(a|o^f) \cdot \gamma^t r_f(o^f, a) \\ &= \mathbb{E}_{\tau_f \sim \pi} \left[ \sum_{t=0}^{\infty} \gamma^t r_f(o_t^f, a_t) \right], \end{aligned} \quad (32)$$

concluding the proof.  $\square$

## F.2 PROOF OF THEOREM 4.4

**Theorem 4.4.** *Given any two policies,  $\tilde{\pi}$  and  $\pi$ , the following bound holds:*

$$\begin{aligned} \zeta(\tilde{\pi}) &\geq L_\pi(\tilde{\pi}) - \frac{2r_{\max}(1-Z)}{1-\gamma} - \frac{2\gamma\epsilon_{\text{train}}}{(1-\gamma)^2} \mathbb{E}_{\substack{f \sim p_{\text{train}}(\cdot) \\ s \sim d^{\mu_f}(\cdot)}} [D_{\text{TV}}(\tilde{\mu}_f \| \mu_f)[s]] \\ &\quad - \frac{2\delta_{\text{train}}(1-Z)}{1-\gamma} \mathbb{E}_{\substack{f \sim p_{\text{train}}(\cdot) \\ s \sim d^{\tilde{\mu}_f}(\cdot)}} [D_{\text{TV}}(\tilde{\mu}_f \| \mu_f)[s]] - \frac{2\delta_{\text{eval}}(1-Z)}{1-\gamma} \mathbb{E}_{\substack{f \sim p_{\text{eval}}(\cdot) \\ s \sim d^{\tilde{\mu}_f}(\cdot)}} [D_{\text{TV}}(\tilde{\mu}_f \| \mu_f)[s]]. \end{aligned} \quad (33)$$

*Proof.* Let's start with the first-order approximation of the training performance (Schulman et al., 2015), denote it as

$$L_\pi(\tilde{\pi}) = \eta(\pi) + \frac{1}{1-\gamma} \mathbb{E}_{\substack{f \sim p_{\text{train}}(\cdot) \\ s \sim d^{\mu_f}(\cdot) \\ a \sim \tilde{\mu}_f(\cdot|s)}} [A^{\mu_f}(s, a)]. \quad (34)$$

Then, we are trying to bound the difference between  $\zeta(\tilde{\pi})$  and  $L_\pi(\tilde{\pi})$ , according to Lemma F.1, that is,

$$\begin{aligned} &|\zeta(\tilde{\pi}) - L_\pi(\tilde{\pi})| \\ &= \left| \zeta(\pi) - \eta(\pi) + \frac{1}{1-\gamma} \mathbb{E}_{\substack{f \sim p(\cdot) \\ s \sim d^{\mu_f}(\cdot) \\ a \sim \mu_f(\cdot|s)}} [A^{\mu_f}(s, a)] - \frac{1}{1-\gamma} \mathbb{E}_{\substack{f \sim p_{\text{train}}(\cdot) \\ s \sim d^{\mu_f}(\cdot) \\ a \sim \tilde{\mu}_f(\cdot|s)}} [A^{\mu_f}(s, a)] \right| \\ &= \frac{1}{1-\gamma} \left| \mathbb{E}_{\substack{f \sim p(\cdot) \\ s \sim d^{\mu_f}(\cdot) \\ a \sim \mu_f(\cdot|s)}} [r(s, a)] - \mathbb{E}_{\substack{f \sim p_{\text{train}}(\cdot) \\ s \sim d^{\mu_f}(\cdot) \\ a \sim \mu_f(\cdot|s)}} [r(s, a)] + \mathbb{E}_{\substack{f \sim p(\cdot) \\ s \sim d^{\mu_f}(\cdot) \\ a \sim \tilde{\mu}_f(\cdot|s)}} [A^{\mu_f}(s, a)] - \mathbb{E}_{\substack{f \sim p_{\text{train}}(\cdot) \\ s \sim d^{\mu_f}(\cdot) \\ a \sim \tilde{\mu}_f(\cdot|s)}} [A^{\mu_f}(s, a)] \right| \\ &\leq \frac{1}{1-\gamma} \left\{ \left| \mathbb{E}_{\substack{f \sim p(\cdot) \\ s \sim d^{\mu_f}(\cdot) \\ a \sim \mu_f(\cdot|s)}} [r(s, a)] - \mathbb{E}_{\substack{f \sim p_{\text{train}}(\cdot) \\ s \sim d^{\mu_f}(\cdot) \\ a \sim \mu_f(\cdot|s)}} [r(s, a)] \right| + \left| \mathbb{E}_{\substack{f \sim p(\cdot) \\ s \sim d^{\mu_f}(\cdot) \\ a \sim \tilde{\mu}_f(\cdot|s)}} [A^{\mu_f}(s, a)] - \mathbb{E}_{\substack{f \sim p_{\text{train}}(\cdot) \\ s \sim d^{\mu_f}(\cdot) \\ a \sim \tilde{\mu}_f(\cdot|s)}} [A^{\mu_f}(s, a)] \right| \right\}. \end{aligned} \quad (35)$$

We can bound these two terms separately. Simplifying the notation, denote  $g(f) = \mathbb{E}_{s \sim d^{\mu_f}(\cdot), a \sim \mu_f(\cdot|s)} [r(s, a)]$ , we can thus rewrite the first term as

$$\left| \mathbb{E}_{\substack{f \sim p(\cdot) \\ s \sim d^{\mu_f}(\cdot) \\ a \sim \mu_f(\cdot|s)}} [r(s, a)] - \mathbb{E}_{\substack{f \sim p_{\text{train}}(\cdot) \\ s \sim d^{\mu_f}(\cdot) \\ a \sim \mu_f(\cdot|s)}} [r(s, a)] \right| = \left| \mathbb{E}_{f \sim p(\cdot)} [g(f)] - \mathbb{E}_{f \sim p_{\text{train}}(\cdot)} [g(f)] \right|, \quad (36)$$

then

$$\left| \mathbb{E}_{f \sim p(\cdot)} [g(f)] - \mathbb{E}_{f \sim p_{\text{train}}(\cdot)} [g(f)] \right| = \left| \int_{\mathcal{F}} p(f) \cdot g(f) df - \int_{\mathcal{F}_{\text{train}}} p_{\text{train}}(f) \cdot g(f) df \right|. \quad (37)$$

Next, according to Assumption 4.1,

$$\begin{aligned}
& \left| \int_{\mathcal{F}} p(f) \cdot g(f) df - \int_{\mathcal{F}_{\text{train}}} p_{\text{train}}(f) \cdot g(f) df \right| = \left| \int_{\mathcal{F}} p(f) \cdot g(f) df - \int_{\mathcal{F}_{\text{train}}} \frac{p(f)}{Z} \cdot g(f) df \right| \\
&= \left| \int_{\mathcal{F}_{\text{train}}} p(f) \cdot g(f) df - \int_{\mathcal{F}_{\text{train}}} \frac{p(f)}{Z} \cdot g(f) df + \int_{\mathcal{F} - \mathcal{F}_{\text{train}}} p(f) \cdot g(f) df \right| \\
&= \left| \int_{\mathcal{F}_{\text{train}}} \frac{Z-1}{Z} p(f) \cdot g(f) df + \int_{\mathcal{F} - \mathcal{F}_{\text{train}}} p(f) \cdot g(f) df \right|,
\end{aligned} \tag{38}$$

where  $Z = \int_{\mathcal{F}_{\text{train}}} p(f) df \leq 1$ , thus,

$$\begin{aligned}
& \left| \int_{\mathcal{F}_{\text{train}}} \frac{Z-1}{Z} p(f) \cdot g(f) df + \int_{\mathcal{F} - \mathcal{F}_{\text{train}}} p(f) \cdot g(f) df \right| \\
& \leq \left| \int_{\mathcal{F}_{\text{train}}} \frac{Z-1}{Z} p(f) \cdot g(f) df \right| + \left| \int_{\mathcal{F} - \mathcal{F}_{\text{train}}} p(f) \cdot g(f) df \right| \\
& \leq \frac{1-Z}{Z} \left| \int_{\mathcal{F}_{\text{train}}} p(f) \cdot g(f) df \right| + \left| \int_{\mathcal{F} - \mathcal{F}_{\text{train}}} p(f) \cdot g(f) df \right|. \tag{39}
\end{aligned}$$

Meanwhile,

$$\begin{aligned}
|g(f)| &= \left| \mathbb{E}_{\substack{s \sim d^{\mu_f}(\cdot) \\ a \sim \mu_f(\cdot|s)}} [r(s, a)] \right| = \left| \sum_{s \in \mathcal{S}} (1 - \gamma) \sum_{t=0}^{\infty} \gamma^t \mathbb{P}(s_t = s | \mu_f) \sum_{a \in \mathcal{A}} \mu_f(a|s) \cdot r(s, a) \right| \\
&\leq (1 - \gamma) \sum_{t=0}^{\infty} \sum_{s \in \mathcal{S}} \mathbb{P}(s_t = s | \mu_f) \sum_{a \in \mathcal{A}} \mu_f(a|s) \cdot \gamma^t |r(s, a)| \\
&\leq (1 - \gamma) \sum_{t=0}^{\infty} \gamma^t r_{\max} = r_{\max},
\end{aligned} \tag{40}$$

where  $r_{\max} = \max_{s,a} |r(s,a)|$ , then we can bound the first term as

$$\begin{aligned}
& \left| \mathbb{E}_{\substack{f \sim p(\cdot) \\ s \sim d^{\mu_f}(\cdot) \\ a \sim \mu_f(\cdot | s)}} [r(s, a)] - \mathbb{E}_{\substack{f \sim p_{\text{train}}(\cdot) \\ s \sim d^{\mu_f}(\cdot) \\ a \sim \mu_f(\cdot | s)}} [r(s, a)] \right| \leq \frac{1-Z}{Z} \left| \int_{\mathcal{F}_{\text{train}}} p(f) \cdot g(f) df \right| + \left| \int_{\mathcal{F} - \mathcal{F}_{\text{train}}} p(f) \cdot g(f) df \right| \\
& \leq \frac{1-Z}{Z} \int_{\mathcal{F}_{\text{train}}} p(f) \cdot |g(f)| df + \int_{\mathcal{F} - \mathcal{F}_{\text{train}}} p(f) \cdot |g(f)| df \\
& \leq \frac{(1-Z)r_{\max}}{Z} \int_{\mathcal{F}_{\text{train}}} p(f) df + r_{\max} \int_{\mathcal{F} - \mathcal{F}_{\text{train}}} p(f) df \\
& = \frac{(1-Z)r_{\max}}{Z} \cdot Z + r_{\max} \cdot (1-Z) = 2r_{\max}(1-Z).
\end{aligned} \tag{41}$$

Now we are trying to bound the second term, which can be expressed as

$$\begin{aligned}
& \left| \mathbb{E}_{\substack{f \sim p(\cdot) \\ s \sim d^{\tilde{\mu}_f}(\cdot) \\ a \sim \tilde{\mu}_f(\cdot|s)}} [A^{\mu_f}(s, a)] - \mathbb{E}_{\substack{f \sim p_{\text{train}}(\cdot) \\ s \sim d^{\mu_f}(\cdot) \\ a \sim \tilde{\mu}_f(\cdot|s)}} [A^{\mu_f}(s, a)] \right| \\
&= \left| \mathbb{E}_{\substack{f \sim p(\cdot) \\ s \sim d^{\tilde{\mu}_f}(\cdot) \\ a \sim \tilde{\mu}_f(\cdot|s)}} [A^{\mu_f}(s, a)] - \mathbb{E}_{\substack{f \sim p_{\text{train}}(\cdot) \\ s \sim d^{\tilde{\mu}_f}(\cdot) \\ a \sim \tilde{\mu}_f(\cdot|s)}} [A^{\mu_f}(s, a)] + \mathbb{E}_{\substack{f \sim p_{\text{train}}(\cdot) \\ s \sim d^{\tilde{\mu}_f}(\cdot) \\ a \sim \tilde{\mu}_f(\cdot|s)}} [A^{\mu_f}(s, a)] - \mathbb{E}_{\substack{f \sim p_{\text{train}}(\cdot) \\ s \sim d^{\mu_f}(\cdot) \\ a \sim \tilde{\mu}_f(\cdot|s)}} [A^{\mu_f}(s, a)] \right| \\
&\leq \underbrace{\left| \mathbb{E}_{\substack{f \sim p(\cdot) \\ s \sim d^{\tilde{\mu}_f}(\cdot) \\ a \sim \tilde{\mu}_f(\cdot|s)}} [A^{\mu_f}(s, a)] - \mathbb{E}_{\substack{f \sim p_{\text{train}}(\cdot) \\ s \sim d^{\tilde{\mu}_f}(\cdot) \\ a \sim \tilde{\mu}_f(\cdot|s)}} [A^{\mu_f}(s, a)] \right|}_{\text{denote as } \Phi} + \underbrace{\left| \mathbb{E}_{\substack{f \sim p_{\text{train}}(\cdot) \\ s \sim d^{\tilde{\mu}_f}(\cdot) \\ a \sim \tilde{\mu}_f(\cdot|s)}} [A^{\mu_f}(s, a)] - \mathbb{E}_{\substack{f \sim p_{\text{train}}(\cdot) \\ s \sim d^{\mu_f}(\cdot) \\ a \sim \tilde{\mu}_f(\cdot|s)}} [A^{\mu_f}(s, a)] \right|}_{\text{denote as } \Psi}.
\end{aligned} \tag{42}$$

Using Corollary F.4,  $\Psi$  can be bounded by

$$\begin{aligned}
\Psi &= \left| \mathbb{E}_{f \sim p_{\text{train}}(\cdot)} \left\{ \mathbb{E}_{\substack{s \sim d^{\tilde{\mu}_f}(\cdot) \\ a \sim \tilde{\mu}_f(\cdot|s)}} [A^{\mu_f}(s, a)] - \mathbb{E}_{\substack{s \sim d^{\mu_f}(\cdot) \\ a \sim \tilde{\mu}_f(\cdot|s)}} [A^{\mu_f}(s, a)] \right\} \right| \\
&\leq \mathbb{E}_{f \sim p_{\text{train}}(\cdot)} \left\{ \left| \mathbb{E}_{\substack{s \sim d^{\tilde{\mu}_f}(\cdot) \\ a \sim \tilde{\mu}_f(\cdot|s)}} [A^{\mu_f}(s, a)] - \mathbb{E}_{\substack{s \sim d^{\mu_f}(\cdot) \\ a \sim \tilde{\mu}_f(\cdot|s)}} [A^{\mu_f}(s, a)] \right| \right\} \\
&\leq \mathbb{E}_{f \sim p_{\text{train}}(\cdot)} \left\{ \frac{2\epsilon\gamma}{1-\gamma} \mathbb{E}_{s \sim d^{\mu_f}(\cdot)} [D_{\text{TV}}(\tilde{\mu}_f \| \mu_f)[s]] \right\},
\end{aligned} \tag{43}$$

where  $\epsilon = \max_s |\mathbb{E}_{a \sim \tilde{\mu}_f(\cdot|s)} [A^{\mu_f}(s, a)]|$ , denote  $\epsilon_{\text{train}} = \max_{f \in \mathcal{F}_{\text{train}}} \{\epsilon\}$ , we obtain

$$\Psi \leq \frac{2\gamma\epsilon_{\text{train}}}{1-\gamma} \mathbb{E}_{\substack{f \sim p_{\text{train}}(\cdot) \\ s \sim d^{\mu_f}(\cdot)}} [D_{\text{TV}}(\tilde{\mu}_f \| \mu_f)[s]]. \tag{44}$$

Next, with a little abuse of notation  $g(f)$ , denote

$$g(f) = \mathbb{E}_{\substack{s \sim d^{\tilde{\mu}_f}(\cdot) \\ a \sim \tilde{\mu}_f(\cdot|s)}} [A^{\mu_f}(s, a)], \tag{45}$$

we can rewrite  $\Phi$  as

$$\Phi = \left| \mathbb{E}_{f \sim p(\cdot)} [g(f)] - \mathbb{E}_{f \sim p_{\text{train}}(\cdot)} [g(f)] \right|, \tag{46}$$

then, similar to (37), (38), (39) and (41),

$$\Phi \leq \frac{1-Z}{Z} \int_{\mathcal{F}_{\text{train}}} p(f) \cdot |g(f)| \, df + \int_{\mathcal{F} - \mathcal{F}_{\text{train}}} p(f) \cdot |g(f)| \, df. \tag{47}$$

According to Lemma F.3, we can bound  $g(f)$ , which can be expressed as

$$g(f) = \mathbb{E}_{\substack{s \sim d^{\tilde{\mu}_f}(\cdot) \\ a \sim \tilde{\mu}_f(\cdot|s)}} [A^{\mu_f}(s, a)] = \mathbb{E}_{s \sim d^{\tilde{\mu}_f}(\cdot)} \left\{ \mathbb{E}_{a \sim \tilde{\mu}_f(\cdot|s)} [A^{\mu_f}(s, a)] \right\}, \tag{48}$$

1296 thus,

$$1298 |g(f)| \leq \mathbb{E}_{s \sim d^{\mu_f}(\cdot)} \left\{ \left| \mathbb{E}_{a \sim \tilde{\mu}_f(\cdot|s)} [A^{\mu_f}(s, a)] \right| \right\} \leq \mathbb{E}_{s \sim d^{\tilde{\mu}_f}(\cdot)} \left\{ 2D_{\text{TV}}(\tilde{\mu}_f \| \mu_f)[s] \cdot \max_a |A^{\mu_f}(s, a)| \right\}. \quad (49)$$

1301 Denote  $\delta = \max_{s, a} |A^{\mu_f}(s, a)|$ , then we have

$$1303 |g(f)| \leq 2\delta \mathbb{E}_{s \sim d^{\tilde{\mu}_f}(\cdot)} [D_{\text{TV}}(\tilde{\mu}_f \| \mu_f)[s]], \quad (50)$$

1305 which means that

$$\begin{aligned} 1306 \Phi &\leq \frac{1-Z}{Z} \int_{\mathcal{F}_{\text{train}}} p(f) \cdot |g(f)| \, df + \int_{\mathcal{F} - \mathcal{F}_{\text{train}}} p(f) \cdot |g(f)| \, df \\ 1308 &\leq \frac{2\delta_{\text{train}}(1-Z)}{Z} \int_{\mathcal{F}_{\text{train}}} p(f) \cdot \mathbb{E}_{s \sim d^{\tilde{\mu}_f}(\cdot)} [D_{\text{TV}}(\tilde{\mu}_f \| \mu_f)[s]] \, df \\ 1310 &\quad + 2\delta_{\text{eval}} \int_{\mathcal{F} - \mathcal{F}_{\text{train}}} p(f) \cdot \mathbb{E}_{s \sim d^{\tilde{\mu}_f}(\cdot)} [D_{\text{TV}}(\tilde{\mu}_f \| \mu_f)[s]] \, df \\ 1312 &= 2\delta_{\text{train}}(1-Z) \int_{\mathcal{F}_{\text{train}}} \frac{p(f)}{Z} \cdot \mathbb{E}_{s \sim d^{\tilde{\mu}_f}(\cdot)} [D_{\text{TV}}(\tilde{\mu}_f \| \mu_f)[s]] \, df \\ 1314 &\quad + 2\delta_{\text{eval}}(1-Z) \int_{\mathcal{F} - \mathcal{F}_{\text{train}}} \frac{p(f)}{1-Z} \cdot \mathbb{E}_{s \sim d^{\tilde{\mu}_f}(\cdot)} [D_{\text{TV}}(\tilde{\mu}_f \| \mu_f)[s]] \, df \\ 1316 &= 2\delta_{\text{train}}(1-Z) \mathbb{E}_{\substack{f \sim p_{\text{train}}(\cdot) \\ s \sim d^{\tilde{\mu}_f}(\cdot)}} [D_{\text{TV}}(\tilde{\mu}_f \| \mu_f)[s]] + 2\delta_{\text{eval}}(1-Z) \mathbb{E}_{\substack{f \sim p_{\text{eval}}(\cdot) \\ s \sim d^{\tilde{\mu}_f}(\cdot)}} [D_{\text{TV}}(\tilde{\mu}_f \| \mu_f)[s]], \end{aligned} \quad (51)$$

1322 where  $\delta_{\text{train}} = \max_{f \in \mathcal{F}_{\text{train}}} \{ \max_{s, a} |A^{\mu_f}(s, a)| \}$  and  $\delta_{\text{eval}} = \max_{f \in \mathcal{F}_{\text{eval}}} \{ \max_{s, a} |A^{\mu_f}(s, a)| \}$ .

1324 Finally, combining (35), (41), (42), (44), and (51), we have

$$\begin{aligned} 1326 |\zeta(\tilde{\pi}) - L_{\pi}(\tilde{\pi})| &\leq \frac{2r_{\max}(1-Z)}{1-\gamma} + \frac{2\gamma\epsilon_{\text{train}}}{(1-\gamma)^2} \mathbb{E}_{\substack{f \sim p_{\text{train}}(\cdot) \\ s \sim d^{\mu_f}(\cdot)}} [D_{\text{TV}}(\tilde{\mu}_f \| \mu_f)[s]] \\ 1328 &\quad + \frac{2\delta_{\text{train}}(1-Z)}{1-\gamma} \mathbb{E}_{\substack{f \sim p_{\text{train}}(\cdot) \\ s \sim d^{\tilde{\mu}_f}(\cdot)}} [D_{\text{TV}}(\tilde{\mu}_f \| \mu_f)[s]] + \frac{2\delta_{\text{eval}}(1-Z)}{1-\gamma} \mathbb{E}_{\substack{f \sim p_{\text{eval}}(\cdot) \\ s \sim d^{\tilde{\mu}_f}(\cdot)}} [D_{\text{TV}}(\tilde{\mu}_f \| \mu_f)[s]], \end{aligned} \quad (52)$$

1332 thus, the generalization performance lower bound is

$$\begin{aligned} 1335 \zeta(\tilde{\pi}) &\geq L_{\pi}(\tilde{\pi}) - \frac{2r_{\max}(1-Z)}{1-\gamma} - \frac{2\gamma\epsilon_{\text{train}}}{(1-\gamma)^2} \mathbb{E}_{\substack{f \sim p_{\text{train}}(\cdot) \\ s \sim d^{\mu_f}(\cdot)}} [D_{\text{TV}}(\tilde{\mu}_f \| \mu_f)[s]] \\ 1337 &\quad - \frac{2\delta_{\text{train}}(1-Z)}{1-\gamma} \mathbb{E}_{\substack{f \sim p_{\text{train}}(\cdot) \\ s \sim d^{\tilde{\mu}_f}(\cdot)}} [D_{\text{TV}}(\tilde{\mu}_f \| \mu_f)[s]] - \frac{2\delta_{\text{eval}}(1-Z)}{1-\gamma} \mathbb{E}_{\substack{f \sim p_{\text{eval}}(\cdot) \\ s \sim d^{\tilde{\mu}_f}(\cdot)}} [D_{\text{TV}}(\tilde{\mu}_f \| \mu_f)[s]], \end{aligned} \quad (53)$$

1342 concluding the proof.  $\square$

### 1344 F.3 PROOF OF THEOREM 4.3

1346 **Theorem 4.3.** *Given any two policies,  $\tilde{\pi}$  and  $\pi$ , the following bound holds:*

$$1347 \eta(\tilde{\pi}) \geq L_{\pi}(\tilde{\pi}) - \frac{2\gamma\epsilon_{\text{train}}}{(1-\gamma)^2} \mathbb{E}_{\substack{f \sim p_{\text{train}}(\cdot) \\ s \sim d^{\mu_f}(\cdot)}} [D_{\text{TV}}(\tilde{\mu}_f \| \mu_f)[s]]. \quad (54)$$

*Proof.* Since

$$\begin{aligned}
|\eta(\tilde{\pi}) - L_\pi(\tilde{\pi})| &= \frac{1}{1-\gamma} \left| \mathbb{E}_{\substack{f \sim p_{\text{train}}(\cdot) \\ s \sim d^{\tilde{\mu}_f}(\cdot) \\ a \sim \tilde{\mu}_f(\cdot|s)}} [A^{\mu_f}(s, a)] - \mathbb{E}_{\substack{f \sim p_{\text{train}}(\cdot) \\ s \sim d^{\mu_f}(\cdot) \\ a \sim \tilde{\mu}_f(\cdot|s)}} [A^{\mu_f}(s, a)] \right| = \frac{\Psi}{1-\gamma} \\
&\leq \frac{2\gamma\epsilon_{\text{train}}}{(1-\gamma)^2} \mathbb{E}_{\substack{f \sim p_{\text{train}}(\cdot) \\ s \sim d^{\mu_f}(\cdot)}} [D_{\text{TV}}(\tilde{\mu}_f \| \mu_f)[s]] ,
\end{aligned} \tag{55}$$

thus,

$$\eta(\tilde{\pi}) \geq L_\pi(\tilde{\pi}) - \frac{2\gamma\epsilon_{\text{train}}}{(1-\gamma)^2} \mathbb{E}_{\substack{f \sim p_{\text{train}}(\cdot) \\ s \sim d_f^{\mu_f}(\cdot)}} [D_{\text{TV}}(\tilde{\mu}_f \| \mu_f)[s]] , \quad (56)$$

concluding the proof.

## F.4 PROOF OF THEOREM 4.5

**Theorem 4.5.** *Given any two policies,  $\tilde{\pi}$  and  $\pi$ , the following bound holds:*

$$\mathfrak{D}_1 \leq \left(1 + \frac{2\gamma\sigma_{\text{train}}}{1-\gamma}\right) \mathfrak{D}_{\text{train}}, \quad \mathfrak{D}_2 \leq \left(1 + \frac{2\gamma\sigma_{\text{eval}}}{1-\gamma}\right) \underbrace{\mathbb{E}_{\substack{f \sim p_{\text{eval}}(\cdot) \\ s \sim d^\mu(\cdot)}} [D_{\text{TV}}(\tilde{\mu}_f \| \mu_f)[s]]}_{\text{denote it as } \mathfrak{D}_{\text{eval}}}, \quad (57)$$

where  $\sigma_{\text{train}} = \max_{f \in \mathcal{F}_{\text{train}}} \{D_{\text{TV}}^{\max}(\tilde{\mu}_f \| \mu_f)[s]\}$  and  $\sigma_{\text{eval}} = \max_{f \in \mathcal{F}_{\text{eval}}} \{D_{\text{TV}}^{\max}(\tilde{\mu}_f \| \mu_f)[s]\}$ ,  $D_{\text{TV}}^{\max}(\tilde{\mu}_f \| \mu_f)[s]$  represents  $\max_s D_{\text{TV}}(\tilde{\mu}_f \| \mu_f)[s]$ .

*Proof.* According to Lemma F.2, we have

$$\begin{aligned}
|\mathfrak{D}_1 - \mathfrak{D}_{\text{train}}| &= \left| \mathbb{E}_{\substack{f \sim p_{\text{train}}(\cdot) \\ s \sim d^{\tilde{\mu}_f}(\cdot)}} [D_{\text{TV}}(\tilde{\mu}_f \| \mu_f)[s]] - \mathbb{E}_{\substack{f \sim p_{\text{train}}(\cdot) \\ s \sim d^{\mu_f}(\cdot)}} [D_{\text{TV}}(\tilde{\mu}_f \| \mu_f)[s]] \right| \\
&= \left| \mathbb{E}_{f \sim p_{\text{train}}(\cdot)} \left\{ \mathbb{E}_{\substack{s \sim d^{\tilde{\mu}_f}(\cdot)}} [D_{\text{TV}}(\tilde{\mu}_f \| \mu_f)[s]] - \mathbb{E}_{\substack{s \sim d^{\mu_f}(\cdot)}} [D_{\text{TV}}(\tilde{\mu}_f \| \mu_f)[s]] \right\} \right| \\
&\leq \mathbb{E}_{f \sim p_{\text{train}}(\cdot)} \left\{ \left| \mathbb{E}_{\substack{s \sim d^{\tilde{\mu}_f}(\cdot)}} [D_{\text{TV}}(\tilde{\mu}_f \| \mu_f)[s]] - \mathbb{E}_{\substack{s \sim d^{\mu_f}(\cdot)}} [D_{\text{TV}}(\tilde{\mu}_f \| \mu_f)[s]] \right| \right\} \\
&\leq \mathbb{E}_{f \sim p_{\text{train}}(\cdot)} \left\{ \left\| d^{\tilde{\mu}_f} - d^{\mu_f} \right\|_1 \cdot \left\| D_{\text{TV}}(\tilde{\mu}_f \| \mu_f)[s] \right\|_{\infty} \right\} \\
&\leq \mathbb{E}_{f \sim p_{\text{train}}(\cdot)} \left\{ \frac{2\gamma}{1-\gamma} \mathbb{E}_{s \sim d^{\mu_f}(\cdot)} [D_{\text{TV}}(\tilde{\mu}_f \| \mu_f)[s]] \cdot \max_s D_{\text{TV}}(\tilde{\mu}_f \| \mu_f)[s] \right\} \\
&\leq \frac{2\gamma\sigma_{\text{train}}}{1-\gamma} \mathbb{E}_{\substack{f \sim p_{\text{train}}(\cdot) \\ s \sim d^{\mu_f}(\cdot)}} [D_{\text{TV}}(\tilde{\mu}_f \| \mu_f)[s]] = \frac{2\gamma\sigma_{\text{train}}}{1-\gamma} \cdot \mathfrak{D}_{\text{train}}, \tag{58}
\end{aligned}$$

as a result

$$\mathfrak{D}_1 \leq \left(1 + \frac{2\gamma\sigma_{\text{train}}}{1 - \gamma}\right) \mathfrak{D}_{\text{train}}. \quad (59)$$

1404 Similarly, using Lemma F.2 again, we have  
 1405

$$\begin{aligned}
 |\mathfrak{D}_2 - \mathfrak{D}_{\text{eval}}| &= \left| \mathbb{E}_{\substack{f \sim p_{\text{eval}}(\cdot) \\ s \sim d^{\mu_f}(\cdot)}} [D_{\text{TV}}(\tilde{\mu}_f \| \mu_f)[s]] - \mathbb{E}_{\substack{f \sim p_{\text{eval}}(\cdot) \\ s \sim d^{\mu_f}(\cdot)}} [D_{\text{TV}}(\tilde{\mu}_f \| \mu_f)[s]] \right| \\
 &= \left| \mathbb{E}_{f \sim p_{\text{eval}}(\cdot)} \left\{ \mathbb{E}_{s \sim d^{\tilde{\mu}_f}(\cdot)} [D_{\text{TV}}(\tilde{\mu}_f \| \mu_f)[s]] - \mathbb{E}_{s \sim d^{\mu_f}(\cdot)} [D_{\text{TV}}(\tilde{\mu}_f \| \mu_f)[s]] \right\} \right| \\
 &\leq \mathbb{E}_{f \sim p_{\text{eval}}(\cdot)} \left\{ \left| \mathbb{E}_{s \sim d^{\tilde{\mu}_f}(\cdot)} [D_{\text{TV}}(\tilde{\mu}_f \| \mu_f)[s]] - \mathbb{E}_{s \sim d^{\mu_f}(\cdot)} [D_{\text{TV}}(\tilde{\mu}_f \| \mu_f)[s]] \right| \right\} \quad (60) \\
 &\leq \mathbb{E}_{f \sim p_{\text{eval}}(\cdot)} \left\{ \|d^{\tilde{\mu}_f} - d^{\mu_f}\|_1 \cdot \|D_{\text{TV}}(\tilde{\mu}_f \| \mu_f)[s]\|_{\infty} \right\} \\
 &\leq \mathbb{E}_{f \sim p_{\text{eval}}(\cdot)} \left\{ \frac{2\gamma}{1-\gamma} \mathbb{E}_{s \sim d^{\mu_f}(\cdot)} [D_{\text{TV}}(\tilde{\mu}_f \| \mu_f)[s]] \cdot \max_s D_{\text{TV}}(\tilde{\mu}_f \| \mu_f)[s] \right\} \\
 &\leq \frac{2\gamma\sigma_{\text{eval}}}{1-\gamma} \mathbb{E}_{\substack{f \sim p_{\text{eval}}(\cdot) \\ s \sim d^{\mu_f}(\cdot)}} [D_{\text{TV}}(\tilde{\mu}_f \| \mu_f)[s]] = \frac{2\gamma\sigma_{\text{eval}}}{1-\gamma} \cdot \mathfrak{D}_{\text{eval}},
 \end{aligned}$$

1423 as a result,

$$\mathfrak{D}_2 \leq \left(1 + \frac{2\gamma\sigma_{\text{eval}}}{1-\gamma}\right) \mathfrak{D}_{\text{eval}}, \quad (61)$$

1424 concluding the proof.  $\square$   
 1425

## 1426 F.5 PROOF OF THEOREM 4.7

1427 **Theorem 4.7.** *Given any two policies,  $\tilde{\pi}$  and  $\pi$ , assume that  $\tilde{\pi}$  is  $\mathcal{R}_{\tilde{\pi}}$ -robust, and  $\pi$  is  $\mathcal{R}_{\pi}$ -robust, then the following bound holds:*

$$\mathfrak{D}_{\text{eval}} \leq \left(1 + \frac{2\gamma\sigma_{\text{train}}}{1-\gamma}\right) \mathcal{R}_{\pi} + \mathcal{R}_{\tilde{\pi}} + \mathfrak{D}_{\text{train}}. \quad (62)$$

1436 *Proof.* Let's first rewrite  $\mathfrak{D}_{\text{eval}}$  as

$$\mathfrak{D}_{\text{eval}} = \mathbb{E}_{\substack{\tilde{f} \sim p_{\text{eval}}(\cdot) \\ s \sim d^{\mu_{\tilde{f}}}(\cdot)}} [D_{\text{TV}}(\tilde{\mu}_{\tilde{f}} \| \mu_{\tilde{f}})[s]]. \quad (63)$$

1441 For another  $f \in \mathcal{F}_{\text{train}}$ , by repeatedly using the triangle inequality of the TV distance, we have

$$\begin{aligned}
 \mathfrak{D}_{\text{eval}} &= \mathbb{E}_{\substack{\tilde{f} \sim p_{\text{eval}}(\cdot) \\ s \sim d^{\mu_{\tilde{f}}}(\cdot)}} [D_{\text{TV}}(\tilde{\mu}_{\tilde{f}} \| \mu_{\tilde{f}})[s]] \\
 &\leq \mathbb{E}_{\substack{\tilde{f} \sim p_{\text{eval}}(\cdot) \\ s \sim d^{\mu_{\tilde{f}}}(\cdot)}} \left[ D_{\text{TV}}(\tilde{\mu}_{\tilde{f}} \| \tilde{\mu}_f)[s] + D_{\text{TV}}(\tilde{\mu}_f \| \mu_f)[s] + D_{\text{TV}}(\mu_f \| \mu_{\tilde{f}})[s] \right] \\
 &= \mathbb{E}_{\substack{\tilde{f} \sim p_{\text{eval}}(\cdot) \\ s \sim d^{\mu_{\tilde{f}}}(\cdot)}} [D_{\text{TV}}(\tilde{\mu}_{\tilde{f}} \| \tilde{\mu}_f)[s]] + \mathbb{E}_{\substack{\tilde{f} \sim p_{\text{eval}}(\cdot) \\ s \sim d^{\mu_{\tilde{f}}}(\cdot)}} [D_{\text{TV}}(\tilde{\mu}_f \| \mu_f)[s]] + \mathbb{E}_{\substack{\tilde{f} \sim p_{\text{eval}}(\cdot) \\ s \sim d^{\mu_{\tilde{f}}}(\cdot)}} [D_{\text{TV}}(\mu_f \| \mu_{\tilde{f}})[s]],
 \end{aligned} \quad (64)$$

1453 taking the expectation of both sides of the inequality with respect to  $f \sim p_{\text{train}}(\cdot)$ , we obtain

$$\mathbb{E}_{f \sim p_{\text{train}}(\cdot)} [\mathfrak{D}_{\text{eval}}] \leq \mathbb{E}_{\substack{f \sim p_{\text{train}}(\cdot) \\ \tilde{f} \sim p_{\text{eval}}(\cdot) \\ s \sim d^{\mu_{\tilde{f}}}(\cdot)}} [D_{\text{TV}}(\tilde{\mu}_{\tilde{f}} \| \tilde{\mu}_f)[s]] + \mathbb{E}_{\substack{f \sim p_{\text{train}}(\cdot) \\ \tilde{f} \sim p_{\text{eval}}(\cdot) \\ s \sim d^{\mu_{\tilde{f}}}(\cdot)}} [D_{\text{TV}}(\tilde{\mu}_f \| \mu_f)[s]] + \mathbb{E}_{\substack{f \sim p_{\text{train}}(\cdot) \\ \tilde{f} \sim p_{\text{eval}}(\cdot) \\ s \sim d^{\mu_{\tilde{f}}}(\cdot)}} [D_{\text{TV}}(\mu_f \| \mu_{\tilde{f}})[s]]. \quad (65)$$

1458 Since  $\mathfrak{D}_{\text{eval}}$  is independent of  $f$ , it becomes a constant after taking the expectation, which is  
 1459

$$1460 \mathfrak{D}_{\text{eval}} \leq \mathbb{E}_{\substack{f \sim p_{\text{train}}(\cdot) \\ \tilde{f} \sim p_{\text{eval}}(\cdot) \\ s \sim d^{\mu_{\tilde{f}}}(\cdot)}} [D_{\text{TV}}(\tilde{\mu}_{\tilde{f}} \parallel \tilde{\mu}_f)[s]] + \mathbb{E}_{\substack{f \sim p_{\text{train}}(\cdot) \\ \tilde{f} \sim p_{\text{eval}}(\cdot) \\ s \sim d^{\mu_f}(\cdot)}} [D_{\text{TV}}(\tilde{\mu}_f \parallel \mu_f)[s]] + \mathbb{E}_{\substack{f \sim p_{\text{train}}(\cdot) \\ \tilde{f} \sim p_{\text{eval}}(\cdot) \\ s \sim d^{\mu_{\tilde{f}}}(\cdot)}} [D_{\text{TV}}(\mu_f \parallel \mu_{\tilde{f}})[s]]. \quad (66)$$

1463  
 1464 Note that  $\tilde{\pi}$  is  $\mathcal{R}_{\tilde{\pi}}$ -robust, and  $\pi$  is  $\mathcal{R}_{\pi}$ -robust, we can thus bound the first term:  
 1465

$$1466 \mathbb{E}_{\substack{f \sim p_{\text{train}}(\cdot) \\ \tilde{f} \sim p_{\text{eval}}(\cdot) \\ s \sim d^{\mu_{\tilde{f}}}(\cdot)}} [D_{\text{TV}}(\tilde{\mu}_{\tilde{f}} \parallel \tilde{\mu}_f)[s]] = \mathbb{E}_{\substack{f \sim p_{\text{train}}(\cdot) \\ \tilde{f} \sim p_{\text{eval}}(\cdot)}} \left[ \sum_{s \in \mathcal{S}} d^{\mu_{\tilde{f}}}(s) \cdot D_{\text{TV}}(\tilde{\mu}_{\tilde{f}} \parallel \tilde{\mu}_f)[s] \right] \\ 1467 \\ 1468 \leq \mathbb{E}_{\substack{f \sim p_{\text{train}}(\cdot) \\ \tilde{f} \sim p_{\text{eval}}(\cdot)}} \left[ \sum_{s \in \mathcal{S}} d^{\mu_{\tilde{f}}}(s) \cdot \mathcal{R}_{\tilde{\pi}} \right] = \mathcal{R}_{\tilde{\pi}} \mathbb{E}_{\substack{f \sim p_{\text{train}}(\cdot) \\ \tilde{f} \sim p_{\text{eval}}(\cdot)}} \left[ \sum_{s \in \mathcal{S}} d^{\mu_{\tilde{f}}}(s) \right] = \mathcal{R}_{\tilde{\pi}}. \quad (67)$$

1469  
 1470 Similarly, we can bound the third term:  
 1471

$$1472 \mathbb{E}_{\substack{f \sim p_{\text{train}}(\cdot) \\ \tilde{f} \sim p_{\text{eval}}(\cdot) \\ s \sim d^{\mu_{\tilde{f}}}(\cdot)}} [D_{\text{TV}}(\mu_{\tilde{f}} \parallel \mu_f)[s]] = \mathbb{E}_{\substack{f \sim p_{\text{train}}(\cdot) \\ \tilde{f} \sim p_{\text{eval}}(\cdot)}} \left[ \sum_{s \in \mathcal{S}} d^{\mu_{\tilde{f}}}(s) \cdot D_{\text{TV}}(\mu_{\tilde{f}} \parallel \mu_f)[s] \right] \\ 1473 \\ 1474 \leq \mathbb{E}_{\substack{f \sim p_{\text{train}}(\cdot) \\ \tilde{f} \sim p_{\text{eval}}(\cdot)}} \left[ \sum_{s \in \mathcal{S}} d^{\mu_{\tilde{f}}}(s) \cdot \mathcal{R}_{\pi} \right] = \mathcal{R}_{\pi} \mathbb{E}_{\substack{f \sim p_{\text{train}}(\cdot) \\ \tilde{f} \sim p_{\text{eval}}(\cdot)}} \left[ \sum_{s \in \mathcal{S}} d^{\mu_{\tilde{f}}}(s) \right] = \mathcal{R}_{\pi}. \quad (68)$$

1475  
 1476 Next, we are trying to bound the second term, which is similar to  $\mathfrak{D}_{\text{train}}$ . Note that  $\mathfrak{D}_{\text{train}}$  is  
 1477 independent of  $\tilde{f}$ , we can thus rewrite it as  
 1478

$$1479 \mathfrak{D}_{\text{train}} = \mathbb{E}_{\substack{f \sim p_{\text{train}}(\cdot) \\ s \sim d^{\mu_f}(\cdot)}} [D_{\text{TV}}(\tilde{\mu}_f \parallel \mu_f)[s]] = \mathbb{E}_{\substack{f \sim p_{\text{train}}(\cdot) \\ \tilde{f} \sim p_{\text{eval}}(\cdot) \\ s \sim d^{\mu_f}(\cdot)}} [D_{\text{TV}}(\tilde{\mu}_f \parallel \mu_f)[s]], \quad (69)$$

1480  
 1481 then  
 1482

$$1483 \left| \mathbb{E}_{\substack{f \sim p_{\text{train}}(\cdot) \\ \tilde{f} \sim p_{\text{eval}}(\cdot) \\ s \sim d^{\mu_{\tilde{f}}}(\cdot)}} [D_{\text{TV}}(\tilde{\mu}_f \parallel \mu_f)[s]] - \mathfrak{D}_{\text{train}} \right| \\ 1484 \\ 1485 = \left| \mathbb{E}_{\substack{f \sim p_{\text{train}}(\cdot) \\ \tilde{f} \sim p_{\text{eval}}(\cdot) \\ s \sim d^{\mu_{\tilde{f}}}(\cdot)}} [D_{\text{TV}}(\tilde{\mu}_f \parallel \mu_f)[s]] - \mathbb{E}_{\substack{f \sim p_{\text{train}}(\cdot) \\ \tilde{f} \sim p_{\text{eval}}(\cdot) \\ s \sim d^{\mu_f}(\cdot)}} [D_{\text{TV}}(\tilde{\mu}_f \parallel \mu_f)[s]] \right| \\ 1486 \\ 1487 = \left| \int_{\mathcal{F}_{\text{train}}} p_{\text{train}}(f) \int_{\mathcal{F}_{\text{eval}}} p_{\text{eval}}(\tilde{f}) \left\{ \mathbb{E}_{\substack{s \sim d^{\mu_{\tilde{f}}}(\cdot)}} [D_{\text{TV}}(\tilde{\mu}_f \parallel \mu_f)[s]] - \mathbb{E}_{\substack{s \sim d^{\mu_f}(\cdot)}} [D_{\text{TV}}(\tilde{\mu}_f \parallel \mu_f)[s]] \right\} d\tilde{f} df \right| \\ 1488 \\ 1489 \leq \int_{\mathcal{F}_{\text{train}}} p_{\text{train}}(f) \int_{\mathcal{F}_{\text{eval}}} p_{\text{eval}}(\tilde{f}) \left\{ \mathbb{E}_{\substack{s \sim d^{\mu_{\tilde{f}}}(\cdot)}} [D_{\text{TV}}(\tilde{\mu}_f \parallel \mu_f)[s]] - \mathbb{E}_{\substack{s \sim d^{\mu_f}(\cdot)}} [D_{\text{TV}}(\tilde{\mu}_f \parallel \mu_f)[s]] \right\} d\tilde{f} df. \quad (70)$$

1490  
 1491 Note that,  
 1492

$$1493 \left| \mathbb{E}_{\substack{s \sim d^{\mu_{\tilde{f}}}(\cdot)}} [D_{\text{TV}}(\tilde{\mu}_f \parallel \mu_f)[s]] - \mathbb{E}_{\substack{s \sim d^{\mu_f}(\cdot)}} [D_{\text{TV}}(\tilde{\mu}_f \parallel \mu_f)[s]] \right| \leq \|d^{\mu_{\tilde{f}}} - d^{\mu_f}\|_1 \cdot \|D_{\text{TV}}(\tilde{\mu}_f \parallel \mu_f)[s]\|_{\infty}. \quad (71)$$

1512  
1513

According to Lemma F.2,

1514  
1515

$$\|d^{\mu_{\tilde{f}}} - d^{\mu_f}\|_1 \leq \frac{2\gamma}{1-\gamma} \mathbb{E}_{s \sim d^{\mu_f}(\cdot)} \left[ D_{\text{TV}}(\mu_{\tilde{f}} \parallel \mu_f)[s] \right], \quad (72)$$

1516  
1517 $\pi$  is  $\mathcal{R}_\pi$ -robust, so,1518  
1519  
1520

$$\|d^{\mu_{\tilde{f}}} - d^{\mu_f}\|_1 \leq \frac{2\gamma}{1-\gamma} \mathbb{E}_{s \sim d^{\mu_f}(\cdot)} \left[ D_{\text{TV}}(\mu_{\tilde{f}} \parallel \mu_f)[s] \right] = \frac{2\gamma}{1-\gamma} \sum_{s \in \mathcal{S}} d^{\mu_f}(s) \cdot D_{\text{TV}}(\mu_{\tilde{f}} \parallel \mu_f)[s] \leq \frac{2\gamma}{1-\gamma} \mathcal{R}_\pi. \quad (73)$$

1521

As a result,

1522  
1523  
1524  
1525  
1526  
1527

$$\begin{aligned} & \left| \mathbb{E}_{\substack{f \sim p_{\text{train}}(\cdot) \\ \tilde{f} \sim p_{\text{eval}}(\cdot) \\ s \sim d^{\mu_{\tilde{f}}}(\cdot)}} [D_{\text{TV}}(\tilde{\mu}_f \parallel \mu_f)[s]] - \mathfrak{D}_{\text{train}} \right| \\ & \leq \int_{\mathcal{F}_{\text{train}}} p_{\text{train}}(f) \int_{\mathcal{F}_{\text{eval}}} p_{\text{eval}}(\tilde{f}) \cdot \left\{ \left| \mathbb{E}_{s \sim d^{\mu_{\tilde{f}}}(\cdot)} [D_{\text{TV}}(\tilde{\mu}_f \parallel \mu_f)[s]] - \mathbb{E}_{s \sim d^{\mu_f}(\cdot)} [D_{\text{TV}}(\tilde{\mu}_f \parallel \mu_f)[s]] \right| \right\} d\tilde{f} df \\ & \leq \int_{\mathcal{F}_{\text{train}}} p_{\text{train}}(f) \int_{\mathcal{F}_{\text{eval}}} p_{\text{eval}}(\tilde{f}) \cdot \left\{ \frac{2\gamma}{1-\gamma} \mathcal{R}_\pi \cdot \max_s D_{\text{TV}}(\tilde{\mu}_f \parallel \mu_f)[s] \right\} d\tilde{f} df \\ & = \int_{\mathcal{F}_{\text{train}}} p_{\text{train}}(f) \cdot \left\{ \frac{2\gamma}{1-\gamma} \mathcal{R}_\pi \cdot \max_s D_{\text{TV}}(\tilde{\mu}_f \parallel \mu_f)[s] \right\} \cdot \int_{\mathcal{F}_{\text{eval}}} p_{\text{eval}}(\tilde{f}) d\tilde{f} df \\ & = \int_{\mathcal{F}_{\text{train}}} p_{\text{train}}(f) \cdot \left\{ \frac{2\gamma}{1-\gamma} \mathcal{R}_\pi \cdot \max_s D_{\text{TV}}(\tilde{\mu}_f \parallel \mu_f)[s] \right\} df = \frac{2\gamma}{1-\gamma} \mathcal{R}_\pi \int_{\mathcal{F}_{\text{train}}} p_{\text{train}}(f) \cdot \max_s D_{\text{TV}}(\tilde{\mu}_f \parallel \mu_f)[s] df. \end{aligned} \quad (74)$$

1538

1539  
1540We previously defined  $\sigma_{\text{train}} = \max_{f \in \mathcal{F}_{\text{train}}} \{ \max_s D_{\text{TV}}(\tilde{\mu}_f \parallel \mu_f)[s] \}$ , so that1541  
1542  
1543  
1544  
1545  
1546  
1547  
1548  
1549

$$\begin{aligned} & \left| \mathbb{E}_{\substack{f \sim p_{\text{train}}(\cdot) \\ \tilde{f} \sim p_{\text{eval}}(\cdot) \\ s \sim d^{\mu_{\tilde{f}}}(\cdot)}} [D_{\text{TV}}(\tilde{\mu}_f \parallel \mu_f)[s]] - \mathfrak{D}_{\text{train}} \right| \leq \frac{2\gamma}{1-\gamma} \mathcal{R}_\pi \int_{\mathcal{F}_{\text{train}}} p_{\text{train}}(f) \cdot \max_s D_{\text{TV}}(\tilde{\mu}_f \parallel \mu_f)[s] df \\ & \leq \frac{2\gamma\sigma_{\text{train}}}{1-\gamma} \mathcal{R}_\pi \int_{\mathcal{F}_{\text{train}}} p_{\text{train}}(f) df = \frac{2\gamma\sigma_{\text{train}}}{1-\gamma} \mathcal{R}_\pi, \end{aligned} \quad (75)$$

1550

thus, the second term is bounded by

1551  
1552  
1553  
1554  
1555  
1556

$$\mathbb{E}_{\substack{f \sim p_{\text{train}}(\cdot) \\ \tilde{f} \sim p_{\text{eval}}(\cdot) \\ s \sim d^{\mu_{\tilde{f}}}(\cdot)}} [D_{\text{TV}}(\tilde{\mu}_f \parallel \mu_f)[s]] \leq \frac{2\gamma\sigma_{\text{train}}}{1-\gamma} \mathcal{R}_\pi + \mathfrak{D}_{\text{train}}. \quad (76)$$

Finally, combining (67), (68) and (76), we have

1557  
1558  
1559  
1560  
1561  
1562  
1563  
1564  
1565

$$\mathfrak{D}_{\text{eval}} \leq \left( 1 + \frac{2\gamma\sigma_{\text{train}}}{1-\gamma} \right) \mathcal{R}_\pi + \mathcal{R}_{\tilde{\pi}} + \mathfrak{D}_{\text{train}}, \quad (77)$$

concluding the proof.  $\square$